catalysts

MDPI

Article

Niobium and Zirconium Phosphates as Green and Water-Tolerant Catalysts for the Acid-Catalyzed Valorization of Bio-Based Chemicals and Real Lignocellulosic Biomasses

Claudia Antonetti [1,2,*], Anna Maria Raspolli Galletti [1,2], Domenico Licursi [1,2], Sara Fulignati [1,2], Nicola Di Fidio [1,2], Federica Zanetti [3], Andrea Monti [3], Tommaso Tabanelli [4] and Fabrizio Cavani [4]

[1] Department of Chemistry and Industrial Chemistry, University of Pisa, Via Giuseppe Moruzzi 13, 56124 Pisa, Italy
[2] Consorzio Interuniversitario Reattività Chimica e Catalisi (CIRCC), Via Celso Ulpiani 27, 70126 Bari, Italy
[3] Department of Agricultural and Food Sciences, University of Bologna, Viale G. Fanin 44, 40127 Bologna, Italy
[4] Department of Industrial Chemistry "Toso Montanari", Alma Mater Studiorum University of Bologna, Viale Risorgimento 4, 40136 Bologna, Italy
* Correspondence: claudia.antonetti@unipi.it; Tel.: +39-0502219329

Abstract: Commercial niobium and synthesized zirconium phosphates were tested as water-tolerant heterogeneous acid catalysts in the hydrothermal conversion of different bio-based substrates. Different acid-catalyzed reactions were performed using biomass-derived model compounds and more complex real lignocellulosic biomasses as the substrate. The conversion of glucose and cellulose was preliminarily investigated. Then, a wide plethora of raw lignocellulosic biomasses, such as conifer wood sawdust, Jerusalem artichoke, sorghum, miscanthus, foxtail millet, hemp and *Arundo donax*, were valorized towards the production of water-soluble saccharides, 5-hydroxymethylfurfural (HMF), levulinic acid (LA) and furfural. The different catalytic performances of the two phosphates were explained on the basis of their acid features, total acidity, Brønsted/Lewis acid sites ratio and strength. Moreover, a better insight into their structure–acidity relationship was proposed. The different acid properties of niobium and zirconium phosphates enabled us to tune the reaction towards target products, achieving from glucose maximum HMF and LA yields of 24.4 and 24.0 mol%, respectively. Remarkably, when real Jerusalem artichoke biomass was adopted in the presence of niobium and zirconium phosphate, maximum yields of furanic compounds and cellulose-derived sugars of 12.7 and 50.0 mol%, respectively, were obtained, after only 1 h of reaction. The synthesized hydrolysates, which were found to be rich in C5 and C6 carbohydrates, can be better exploited for the cascade production of more added-value bio-products.

Keywords: niobium phosphate; zirconium phosphate; lignocellulosic biomasses; 5-hydroxymethylfurfural; levulinic acid; sugars; oligomers

Citation: Antonetti, C.; Raspolli Galletti, A.M.; Licursi, D.; Fulignati, S.; Di Fidio, N.; Zanetti, F.; Monti, A.; Tabanelli, T.; Cavani, F. Niobium and Zirconium Phosphates as Green and Water-Tolerant Catalysts for the Acid-Catalyzed Valorization of Bio-Based Chemicals and Real Lignocellulosic Biomasses. *Catalysts* **2022**, *12*, 1189. https://doi.org/10.3390/catal12101189

Academic Editors: Hwai Chyuan Ong, Chia-Hung Su and Hoang Chinh Nguyen

Received: 28 August 2022
Accepted: 3 October 2022
Published: 7 October 2022

1. Introduction

Emerging economies with political and environmental concerns about fossil fuels have spurred research into utilizing biomass as feedstock for the sustainable production of new fuels and chemicals. 5-hydroxymethylfurfural (HMF) [1,2] and levulinic acid (LA) [3,4] are very versatile platform chemicals, usable as building blocks for the synthesis of many added-value bio-fuels [5,6] and bio-chemicals [7,8]. The hydrothermal production of HMF and/or LA from lignocellulosic biomasses involves a multistep complex reaction sequence which, once glucose is formed by the hydrolysis stage, includes: i) the isomerization of glucose to fructose, ii) fructose dehydration to HMF, and iii) HMF ring opening by hydrolysis to LA. In this context, many side reactions occur, mainly as condensations of furanic compounds, to give low-molecular water-soluble and higher-molecular water-insoluble humins [9,10]. Formic acid (FA) is co-produced in equimolar amount, or even

slightly higher than LA within LA synthesis (in this latter case due to the possible side reactions of reactive intermediates) [11,12]. The general pathway of the involved reactions, starting from glucose, is reported in Scheme 1.

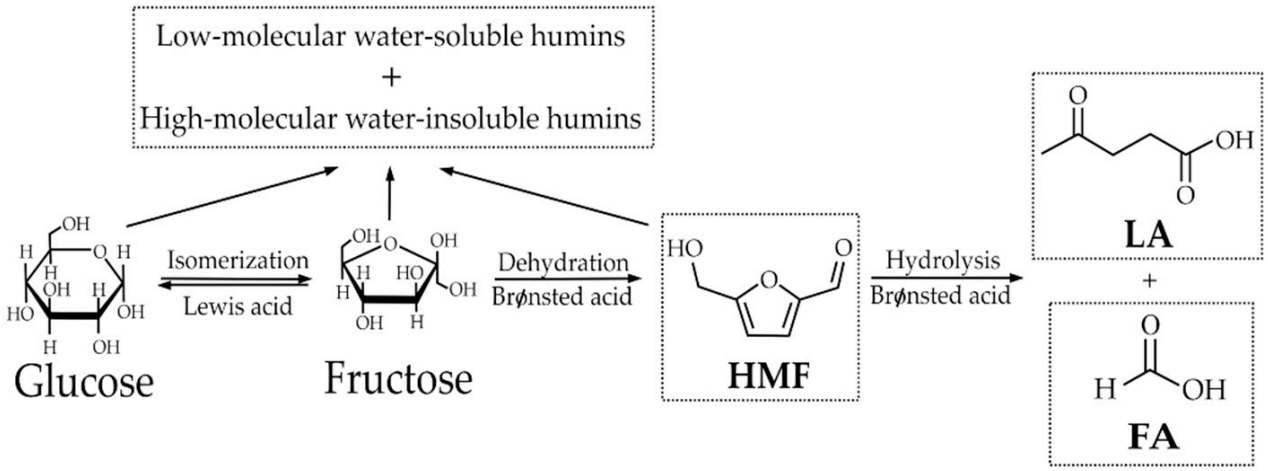

Scheme 1. Reaction pathway of isomerization/dehydration/hydrolysis reactions from glucose to HMF and LA/FA, highlighting the roles of Brønsted/Lewis acids.

Each of these reactions behaves differently, depending on the type and strength of the acid catalyst. Lewis acids selectively favor the first isomerization step of glucose to fructose, whereas Brønsted acids enable the subsequent dehydration/hydrolysis reactions [2,13,14]. Therefore, HMF synthesis requires an accurate tuning both of Brønsted/Lewis acidity and the strength of their acid sites, together with mild reaction conditions of temperature and time, whereas the subsequent HMF hydrolysis to LA needs Brønsted sites and harsher reaction conditions [15,16]. Focusing on HMF production, this compound is traditionally synthesized starting from syrups extracted from energy crops, adopting homogeneous catalysts followed by liquid/liquid extraction with organic solvents [17]. In a similar way, LA production traditionally involves the use of strong inorganic acids, such as HCl and H_2SO_4, as homogeneous catalysts of a two-stage process where LA is first produced and then recovered by stripping [4]. For both HMF and LA processes, the difficult recovery of the homogeneous catalyst, disposal problems and equipment corrosion issues make heterogeneous systems certainly more attractive for industrial applications. Nevertheless, few examples of heterogeneous catalysts for HMF and LA production have been reported in the literature, such as metal oxides, carbon-based catalysts, zeolites, metal–organic frameworks (MOF), resins and metal phosphates [1,2]. Metal oxides [1,18] have low activity and need organic solvents, leading to environmental and economic drawbacks. Similarly, carbon-based catalysts [1,19] show low activity and selectivity, as well as poor stability, resulting in the easy leaching of the active components. On the other hand, zeolites have a good thermal stability, but undergo deactivation by pore blockage as a consequence of the precipitation of various reaction by-products on their surfaces. Moreover, zeolite systems [1,20] generally undergo metal leaching in the aqueous phase, thus resulting in these applications quite unstable. MOFs exhibit high porosity and better tunable reactivity than zeolites, at the same time requiring simpler synthesis procedures. Despite these relevant advantages, synthesized MOFs still show poor thermochemical stability due to the weak coordination bond of the bridged metal [1,21]. Acid resins generally show higher catalytic performances than the above-mentioned catalysts, but their satisfactory recycling is still difficult to achieve, thus making their industrial application unfeasible [1,16]. Finally, metal phosphates, in particular niobium and zirconium phosphates (NbPO and ZrPO), appear to be promising systems, keeping their strong acidic properties even in polar

liquids such as water and at high temperatures. Remarkably, these catalysts can be easily reactivated by simpler thermal treatments [2].

Up to now, few works have reported the use of heterogeneous catalysts for the synthesis of HMF and LA starting from real feedstocks, and their employment is generally limited to the conversion of model substrates, such as soluble sugars or pure cellulose [4]. In this context, Table 1 summarizes the most relevant literature results on the catalytic performances of NbPO and ZrPO towards HMF and LA production in water, starting from model sugars and/or real biomasses.

Table 1. Literature review on HMF and LA production in water catalyzed by NbPO and ZrPO (RAC = substrate/catalyst ratio wt/wt).

Catalyst	Substrate	Product	Reaction Conditions	Product YIeld (mol%)	Reference
NbPO	Fructose	HMF	190 °C, 8 min, RAC 6 wt/wt, 10 wt% loading	32.2	[2]
NbPO	Fructose	HMF	130 °C, 60 min, RAC 1 wt/wt, 4.5 wt% loading	33.6	[22]
NbPO	Glucose	HMF	145 °C, 180 min, RAC 3 wt/wt, 2 wt% loading	15.0	[23]
NbPO	Glucose	HMF	140 °C, 60 min, RAC 1 wt/wt, 4.5 wt% loading	14.1	[22]
NbPO	Glucose	HMF	135 °C, 390 min, RAC 2 wt/wt, 6.2 wt% loading	11.2	[24]
NbPO	Cellobiose	HMF	140 °C, 10 min, RAC 10 wt/wt, 1 wt% loading	6.0	[25]
ZrPO	Fructose	HMF	190 °C, 8 min, RAC 6 wt/wt, 10 wt% loading	39.4	[2]
ZrPO	Glucose	HMF	160 °C, 150 min, RAC 2 wt/wt, 10 wt% loading	15.0	[14]
ZrPO	Glucose	HMF	155 °C, 360 min, RAC 2 wt/wt, 0.5 wt% loading	46.6	[26]
ZrPO	Glucose	LA	160 °C, 150 min, RAC 2 wt/wt, 10 wt% loading	14.0	[14]
ZrPO	Food waste	HMF	160°C, 360 min, RAC 2 wt/wt, 4 wt% loading	4.3 [a]	[27]

[a] Yield expressed as weight % with respect to biomass dry weight due to the absence of the cellulose content in the biomass.

In this work, the catalytic performances of NbPO and ZrPO have been evaluated for several acid-catalyzed hydrolysis/isomerization/dehydration reactions, starting not only from model glucose and cellulose, but also from real lignocellulosic biomasses, such as conifer wood sawdust, Jerusalem artichoke, sorghum, miscanthus, foxtail millet, hemp and *Arundo donax*. In this context, the correlation between the Brønsted/Lewis acidity of NbPO and ZrPO and their catalytic performances has been investigated, especially clarifying the acidity role and structural modifications which phosphates may undergo in the water medium. Moreover, starting from glucose, the optimization of HMF and LA synthesis with NbPO and ZrPO has been carried out. On the other hand, starting from raw lignocellulosic biomasses and employing the same phosphates, it is possible to easily access the plant tissue and selectively produce furanic compounds (HMF and furfural) or cellulose-derived sugars which can be further converted into a plethora of more added-value products within the biomass supply chain. The proposed approach, in particular the employment of these phosphates for the one-pot conversion of low-cost substrates, represents a preliminary but

necessary step towards heterogeneously catalyzed biomass conversion from the perspective of the development of these processes on a greater industrial scale.

2. Results and Discussion

2.1. Conversion of Glucose in the Presence of NbPO and ZrPO

Commercial NbPO and synthesized ZrPO were tested for the conversion of glucose in water. These systems are characterized by the presence of both Brønsted and Lewis acid sites and they were already successfully adopted by us for the microwave (MW)-assisted dehydration of fructose and inulin to HMF [2]. Table 2 summarizes the acid properties of NbPO and ZrPO under the hydrous conditions studied in previous research [2].

Table 2. Acid properties of NbPO and ZrPO under hydrous conditions [2].

	Total Acidity (mmol/g) [a]	**Brønsted/Lewis Ratio** [b]
NbPO	0.33	1.0
ZrPO	0.43	0.2

[a] Determined by NH_3-TPD analysis; [b] values at 200 °C obtained from FT-IR spectra recorded at increasing temperature after room-temperature co-adsorption of pyridine and water.

The dehydration of fructose to HMF reaction requires Brønsted acidity, whereas both Lewis and Brønsted acidities are necessary when glucose is employed as substrate and their balance, in terms of the number and strength of the acid sites, is of paramount importance. In fact, the transformation of glucose to HMF is characterized by a complex network of reactions which are differently promoted by Lewis or Brønsted acid sites. On this basis, the study of the different behaviors of these two systems in aqueous medium is of particular interest.

Firstly, the reaction has been investigated in the autoclave reactor at the temperature of 150 °C, adopting the glucose loading of 5 wt% and the glucose/catalyst weight ratio of 1.2, selected on the basis of preliminary tests (not reported). The obtained results are shown in Figure 1. NbPO shows higher glucose conversion than ZrPO, and this can be justified considering that NbPO in aqueous media is characterized by a higher amount of Brønsted acid sites which promote the dehydration/hydrolysis reaction. In particular, they can boost the fructose dehydration to HMF and, as consequence, foster the isomerization equilibrium from glucose towards fructose, thus improving the glucose conversion. Regarding the products' distribution, in a short reaction time, NbPO shows a relatively high selectivity and yield towards HMF, whereas ZrPO reveals a marked selectivity towards fructose. This can be explained considering the different types of catalysts' acid properties [2]. In fact, in water, NbPO has fewer Lewis centers and a larger amount of Brønsted ones than ZrPO, but all of them are characterized by high acid strength. The peculiar balance of these acid centers allows us to obtain the selective formation of HMF with NbPO. In fact, the Lewis centers boost the isomerization of glucose to fructose, whereas the Brønsted ones favor the subsequent dehydration of fructose to HMF. As consequence, the isomerization of glucose to fructose is further enhanced and HMF selectivity higher than 60 mol% is achieved at the beginning of the reaction (30 min). On the other hand, ZrPO, under the same aqueous conditions, is characterized by a higher concentration of acid sites with a predominant Lewis nature (Table 2), allowing a higher selectivity in fructose at the beginning of the reaction.

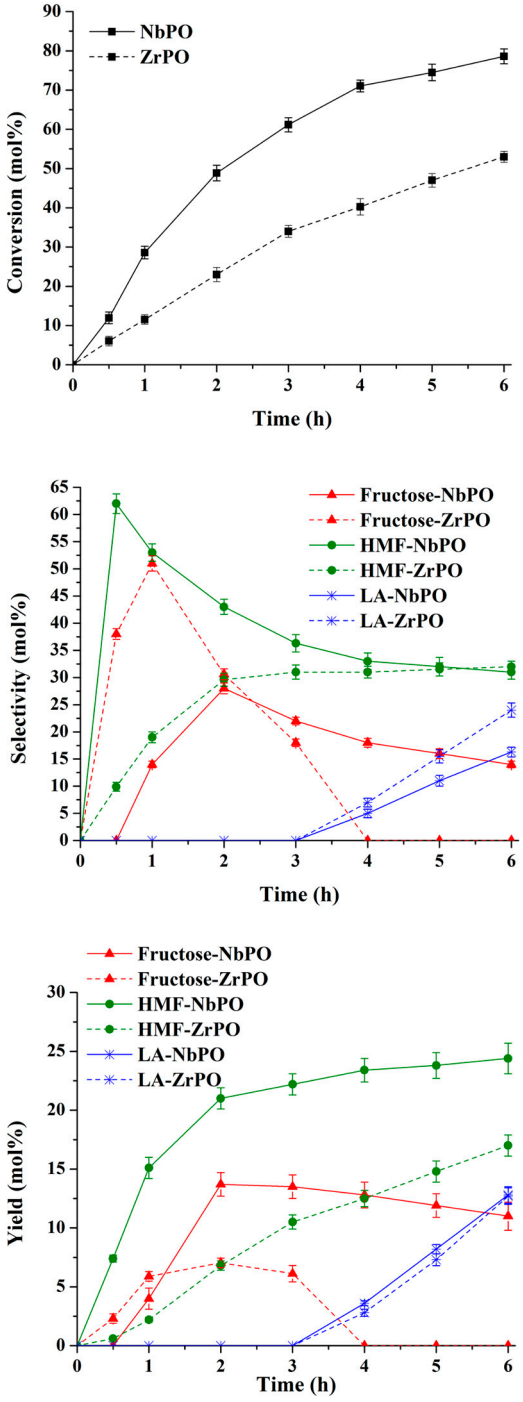

Figure 1. Glucose conversion in the presence of NbPO and ZrPO as acid catalysts in autoclave at 150 °C. Reaction conditions: glucose = 2.47 g; catalyst = 2.06 g; water = 47.0 g; T = 150 °C. Note: where the error bars are not visible, they are smaller than the symbols.

Moreover, it is interesting to note the different behavior of the two systems in the range 1–3 h. When NbPO is employed, a significant decrease in HMF selectivity occurs without the simultaneous production of LA, thus indicating the formation of humins, as confirmed by the corresponding lower %C recovered (mol%). On the other hand, in the presence of ZrPO, HMF selectivity increased and a scarce production of humins took place, as confirmed by the higher %C recovered (mol%) for ZrPO (after 3 h, the %C recovered results were 74.5 and 82.6 mol% for NbPO and ZrPO, respectively). For both phosphates, the prolonging of the reaction time favors the conversion of HMF to LA, due to the presence

of Brønsted acid sites, with comparable LA yields after 6 h of reaction (12.7 mol%). These results highlight that the kinetics of NbPO and ZrPO are different: NbPO is more active and more selective towards HMF in the short reaction time, due to the equal amount of Brønsted and Lewis acid sites that promote the conversion of glucose to HMF through fructose. On the other hand, ZrPO, which is characterized by predominant Lewis acidity, led to a slower conversion and higher fructose selectivity in the short reaction time. The achieved catalytic performances indicate commercial NbPO as a suitable system for the production of HMF, reaching the HMF yield of 22.2 mol% after only 3 h of reaction and the highest HMF yield of 24.4 mol% after 6 h; these values are higher than those reported in the literature for analogous systems in aqueous medium [1,22,23,28]. In fact, working in pure water, which leads to a high decomposition of the formed HMF [28], Ordomsky et al. obtained HMF yields below 10 mol%, working with the same NbPO system at 135 °C and adopting the glucose loading of 5 wt% [24]. The same authors reached the highest selectivity to HMF equal to 56 mol% at 20 mol% glucose conversion in the presence of a synthesized NbPO with a Brønsted/Lewis acid sites ratio equal to 1 [24], the same acid ratio of the commercial NbPO adopted in our experimental conditions where the maximum HMF selectivity resulted in 62.5 mol% at 11.9 mol% glucose conversion. Moreover, they studied the catalytic performances of various synthesized metal phosphates in glucose transformation to HMF, whose performances followed the order: aluminum < titanium < zirconium < niobium phosphate, in agreement with the increase in the strength of their acid sites. The excess of Lewis acid sites caused the excessive formation of undesired humins, leading to significant catalyst deactivation. The authors proposed that the synergism between a protonated phosphate group and a nearby metal Lewis acid site in the two-stage glucose transformation into HMF led to highly selective glucose isomerization/dehydration, whereas an excess of Lewis acidity favored the undesired conversion of glucose into humins, decreasing the selectivity to HMF. These considerations on the Brønsted/Lewis acidity of the phosphates derive from FT-IR experiments carried out through the adsorption of pyridine, but the authors do not consider the effect of water on the catalytic properties of the phosphates. From this perspective, Antonetti et al. [2] studied the Brønsted/Lewis acidity of NbPO and ZrPO when pyridine and water were co-adsorbed and compared the achieved results to the case of pyridine-only adsorption. Working under hydrous conditions, the authors proved that a significant increase in the Brønsted/Lewis ratio occurred for the NbPO system, whereas only a minor variation in the Brønsted/Lewis intensity ratio was observed for ZrPO. Furthermore, the new Brønsted sites generated on the NbPO surface by water adsorption had comparatively higher strength, thus making this system (under hydrous conditions) a strong Brønsted-type acid system. On the other hand, under the same hydrous conditions, ZrPO acid sites remained mainly of the Lewis type, together with Brønsted sites of comparatively lower strength, changing the acid features little. Comparable results to Ordomsky et al. were also obtained by De Jesus Junior et al. [23], who studied the conversion of 2 wt% aqueous solution of glucose to HMF in the presence of the commercial NbPO, achieving the highest HMF yield equal to 15 mol% at 145 °C after 3 h of reaction. Moving towards synthesized NbPO, higher HMF yields up to 33.6 mol% were obtained from 4.8 wt% glucose aqueous solution in pure water, adopting a porous NbPO catalyst synthesized at pH = 7 working at 140 °C for 1 h [22]. Moreover, it was found that an excess of Brønsted acid sites could inhibit the isomerization of glucose to fructose, which is a Lewis acid-promoted process, but boosts the subsequent fructose conversion. On the other hand, an excess of Lewis acidity has a negative influence on the dehydration of fructose, which would lead to undesired side effects with the subsequent formation of humins [13,22]. NbPO prepared at pH = 7 showed the best catalytic performance, achieving HMF selectivity up to 50 mol%, starting from glucose, under the best reaction conditions. In addition, this synthesized catalyst exhibited excellent stability, with almost no decrease in activity and/or selectivity, even after seven successive runs [22]. Moving to ZrPO, on the basis of the achieved results in our work,, it can be considered a promising catalyst for the production of LA, thanks to its higher selectivity to LA compared to NbPO (Figure 1)

and the %C recovered (mol%). Thus, in order to confirm this behaviour and increase the production of LA, ZrPO was tested at 180 °C under the same reaction conditions, as reported in Figure 2.

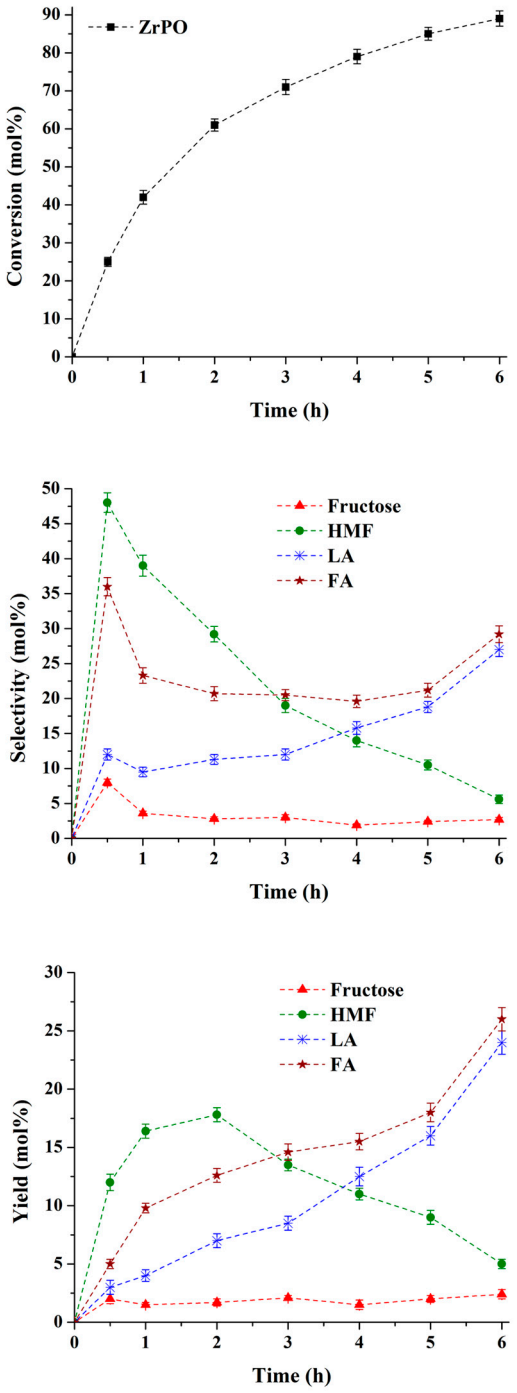

Figure 2. Glucose conversion in the presence of ZrPO as acid catalysts in autoclave at 180 °C. Reaction conditions: glucose = 2.49 g; catalyst = 2.02 g; water = 47.0 g; T = 180 °C. Note: where the error bars are not visible, they are smaller than the symbols.

The increase in temperature improves the glucose conversion, which reaches the value of 71 mol% after only 3 h, instead of 53 mol% after 6 h at 150 °C. Moreover, after 1 h of reaction at 180 °C, the selectivity to fructose is lower than that achieved at 150 °C because this last compound has been converted through dehydration to HMF and the latter has been involved in the hydrolysis reaction with the formation of LA and FA, which

resulted the main products after 6 h of reaction. In this case, the LA yield of 24.0 mol% is obtained after 6 h, highlighting that ZrPO is a promising system for the production of LA at the reaction temperature of 180 °C. The faster kinetics with the rise in temperature is also confirmed with the HMF production: at 180 °C, the highest HMF yield equal to 17.8 mol% is achieved after 2 h of reaction, whereas an analogous value was obtained after 6 h at 150 °C. The ascertained highest LA yield with ZrPO is better than that reported in the literature by Weingarten et al. where the ZrPO synthesized according to the same procedure with the P/Zr molar ratio of 2 resulted the best system, achieving the highest LA yield of 14.0 mol% working at 160 °C [14]. To further improve the selective conversion of glucose towards HMF or LA catalyzed by NbPO and ZrPO, respectively, several tests have been performed under MW irradiation. This is an effective and sustainable tool at the laboratory scale for a rapid screening, enabling a higher heating rate than traditional heating systems, homogeneous heat distribution, efficient control and remarkable energy and time saving [6]. Firstly, in order to optimize the HMF production with NbPO, the effect of the temperature and reaction time was considered and optimized, adopting the same glucose/NbPO weight ratio of 1.2 and glucose loading of 5 wt%. The obtained results are reported in Table 3.

Table 3. MW-assisted conversion of glucose carried out in the presence of NbPO catalyst. Reaction conditions: glucose = 0.24 g; catalyst = 0.20 g; water = 4.6 g.

Run	T (°C)	t (min)	Glucose Conversion (mol%)	Fructose Yield (mol%)	HMF Yield (mol%)	LA Yield (mol%)	HMF Sel. (mol%)	%C Recovered (mol%)
1	140	30	40.0	4.3	13.0	1.0	32.5	78.3
2	150	30	36.0	4.6	11.7	0.6	32.5	80.9
3	160	30	54.0	4.0	23.0	1.1	42.6	74.1
4	160	45	64.0	4.0	21.0	4.6	32.8	65.6
5 [a]	160	30	29.0	2.0	2.4	-	8.3	75.4
6	170	30	63.0	4.8	19.7	4.6	31.3	66.1
7	180	30	95.0	3.0	19.0	9.0	20.0	36.0

[a] Blank test carried out in the absence of catalyst.

Preliminary tests performed at low temperatures (100-120 °C, not shown) led mainly to low amounts of isomerization products (fructose) and up to 5 mol% of HMF yield. This result, although modest in terms of yield, is related to the presence of strong Lewis acid sites on NbPO that catalyze glucose isomerization in aqueous environments at such low temperatures. A further increase in temperature up to 140 °C results in 13 mol% HMF yield and only 1 mol% LA after 30 min of reaction (run 1, Table 3). Then, higher temperatures (up to 160 °C) allow improved HMF yields up to 23.0 mol% (runs 2 and 3, Table 3), whereas LA yields reach only 1.1 mol%. At 150 °C, after the same reaction time of 30 min, in the absence of MW (Figure 1), both glucose conversion and HMF yield are lower (glucose conversion 11.9 mol% and HMF yield 7.4 mol%, respectively), evidencing MW as an efficient tool to speed up the reaction [29]. Taking into account that the best HMF yield (23.0 mol%) was achieved working at 160 °C and 30 min of reaction (run 3, Table 3), a new hydrolysis test was carried out at the same reaction temperature, but for a longer reaction time, equal to 45 min (run 4, Table 3). In this case, an almost comparable HMF yield (21.0 mol%) was obtained but, due to the subsequent rehydration of HMF to LA (yield of 4.6 mol%), together with a lower HMF selectivity (32.8 mol%). Under the best reaction conditions (run 3, Table 3), a blank experiment was also carried out (run 5, Table 3) which unequivocally confirmed the key role of the NbPO catalyst for the HMF synthesis. Lastly, higher temperatures were tested (runs 6 and 7, Table 3), showing that these are not appropriate for the HMF synthesis, but rather promoting the consecutive formation of LA (run 7, Table 3). Adopting MW irradiation, it is interesting to note that

the highest HMF yield (23.0 mol%), which is comparable to that obtained working in autoclave and higher than those reported in the literature for analogous systems in aqueous phase [1,22,23,28], was reached after only 30 min, highlighting again the efficiency of MW heating. After having identified the optimal temperature for the HMF synthesis (160 °C) adopting MW irradiation, a more thorough investigation of the kinetics was performed, adopting the same glucose/NbPO weight ratio of 1.2 and glucose loading of 5 wt%, and the corresponding results are shown in Figure 3.

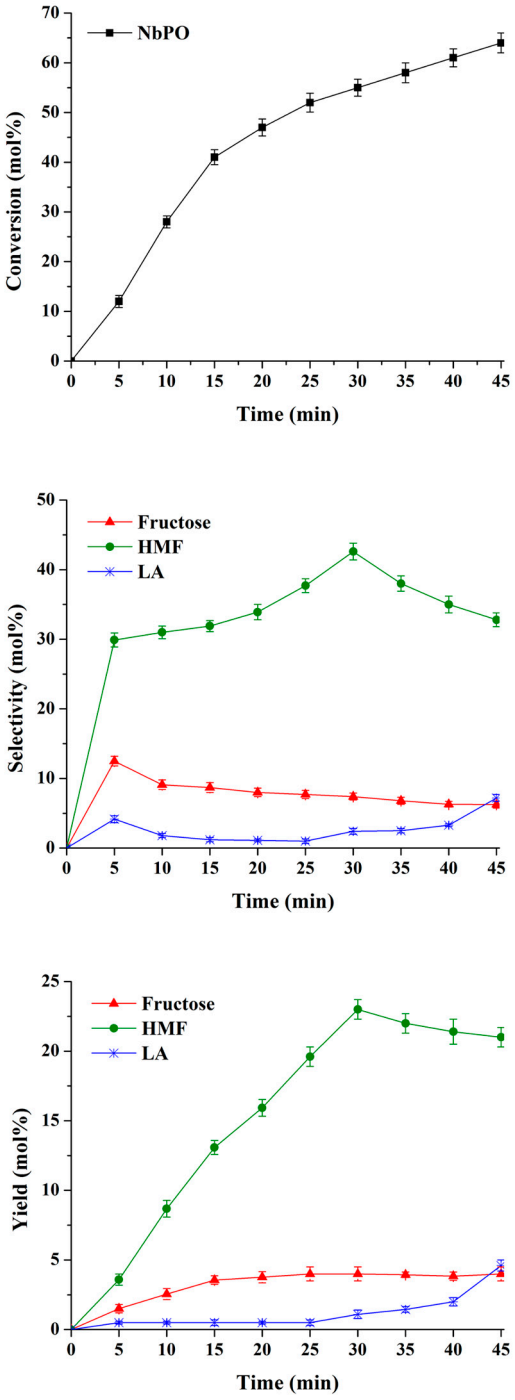

Figure 3. MW-assisted conversion of glucose in the presence of NbPO as acid catalyst at 160 °C. Reaction conditions: glucose = 0.25 g; catalyst = 0.21 g; water = 4.8 g, T = 160 °C. Note: where the error bars are not visible, they are smaller than the symbols.

Figure 3 shows that the highest HMF yield was obtained working at 160 °C after 30 min of reaction, confirming the data already reported in Table 3 (run 3). The selectivity to HMF increases up to 30 min of reaction, when it reaches the maximum value equal to 42.6 mol%, then it slowly decreases as a consequence of the relevant rehydration of HMF to LA with the simultaneous increase in LA selectivity and yield. Starting from the best MW-assisted hydrolysis test to HMF with the NbPO catalyst, ZrPO was also tested under the same reaction conditions (T = 160 °C, glucose/ZrPO weight ratio = 1.2, glucose loading = 5 wt%, t = 30 min). The obtained data with the two catalytic systems are compared in Table 4.

Table 4. MW-assisted conversion of glucose carried out in the presence of ZrPO catalyst. The corresponding hydrolysis experiment with NbPO has been reported for comparison. Reaction conditions: glucose = 0.26 g; catalyst = 0.22 g; water = 5.0 g; T = 160 °C; t = 30 min.

Catalyst	Glucose Conversion (mol%)	Fructose Sel. (mol%)	Fructose Yield (mol%)	HMF Sel. (mol%)	HMF Yield (mol%)	LA Sel. (mol%)	LA Yield (mol%)
NbPO	54.0	7.4	4.0	42.6	23.0	2.0	1.1
ZrPO	41.4	4.8	2.0	23.6	9.8	4.4	1.8

Table 4 highlights that NbPO shows better catalytic performances in terms of conversion, yield and selectivity to HMF than ZrPO, in agreement with the corresponding autoclave tests (Figure 1). On this basis, taking into consideration that ZrPO was active for the production of LA in the longer reaction time, in order to fully exploit the potentialities of ZrPO catalyst for the selective synthesis of LA from glucose, new hydrolysis experiments were carried out under MW irradiation, increasing the reaction temperature up to 190 °C and the reaction time up to 45 min. The results of the MW-assisted experiments are reported in Table 5.

Table 5. MW-assisted conversion of glucose in the presence of ZrPO catalyst at 180 and 190 °C. Reaction conditions: glucose = 0.25 g; catalyst = 0.20 g; water = 4.8 g; t = 45 min.

T (°C)	Glucose Conversion (mol%)	Fructose Sel. (mol%)	Fructose Yield (mol%)	HMF Sel. (mol%)	HMF Yield (mol%)	LA Sel. (mol%)	LA Yield (mol%)
160	49.1	6.1	3.0	36.7	18.0	8.9	4.4
180	54.7	5.6	3.1	32.6	17.8	20.8	11.4
190	72.3	2.4	1.7	23.4	16.9	21.9	15.8

The above data agree with those reported in the literature regarding the effect of temperature on LA synthesis [6], where yield increased from 4.4 to 15.8 mol% from 160 to 190 °C after 45 min.

In summary, starting from glucose, it is possible to highlight that the different acid properties of the two systems NbPO and ZrPO have enabled us to obtain HMF and LA with maximum yields of 24.4 and 24.0 mol%, respectively, (Figures 1 and 2). These values are higher or comparable with those reported in the literature for analogous systems in aqueous phase [1,14,22,23,28]. This is an interesting result because it opens the possibility of studying more complex model substrates, such as untreated cellulose, once having verified the stability and recyclability of the catalysts of interest.

2.2. Catalysts' Stability and Recyclability

Since the stability and the recyclability of the catalysts are of great importance from an applicative and industrial perspective, NbPO and ZrPO were investigated in terms of these

aspects. The NbPO and ZrPO catalysts obtained from the best runs to HMF and LA (run in Figure 1 for NbPO after 6 h and run in Figure 2 for ZrPO after 6 h) were recovered by filtration, washed with acetone and reused within two successive runs performed under the same experimental conditions of the first cycle. The results are reported in Table 6.

Table 6. Glucose conversion in the presence of NbPO (T = 160 °C) and ZrPO (T = 180 °C) under the same reaction conditions (6 h, glucose/catalyst weight ratio = 1.2, glucose loading = 5 wt%) and two subsequent recycles of the solid catalysts.

	Glucose Conversion (mol%)	**HMF Selectivity (mol%)**	**HMF Yield (mol%)**
Fresh NbPO	78.6	31.0	24.4
NbPO used first cycle	76.9	30.2	23.2
NbPO used second cycle	75.5	30.1	22.7
	Glucose Conversion (mol%)	**LA Selectivity (mol%)**	**LA Yield (mol%)**
Fresh ZrPO	89.0	27.0	24.0
ZrPO used first cycle	88.6	27.0	23.9
ZrPO used second cycle	86.3	26.6	23.0

The obtained results confirm the feasibility of catalyst reactivation by simple acetone washing, showing, for both phosphates, only a slight decrease in glucose conversion and HMF/LA selectivities and yields. The good efficiency of the washing suggests that most of the furanic polymers adsorbed on the catalysts' surface are soluble ones, probably derived from condensation reactions.

In order to verify the presence of organic deposits on spent catalysts, FT-IR analyses of NbPO and ZrPO recovered at the end of the best reactions were compared with those of fresh and washed samples. The recorded spectra are shown in Figure 4.

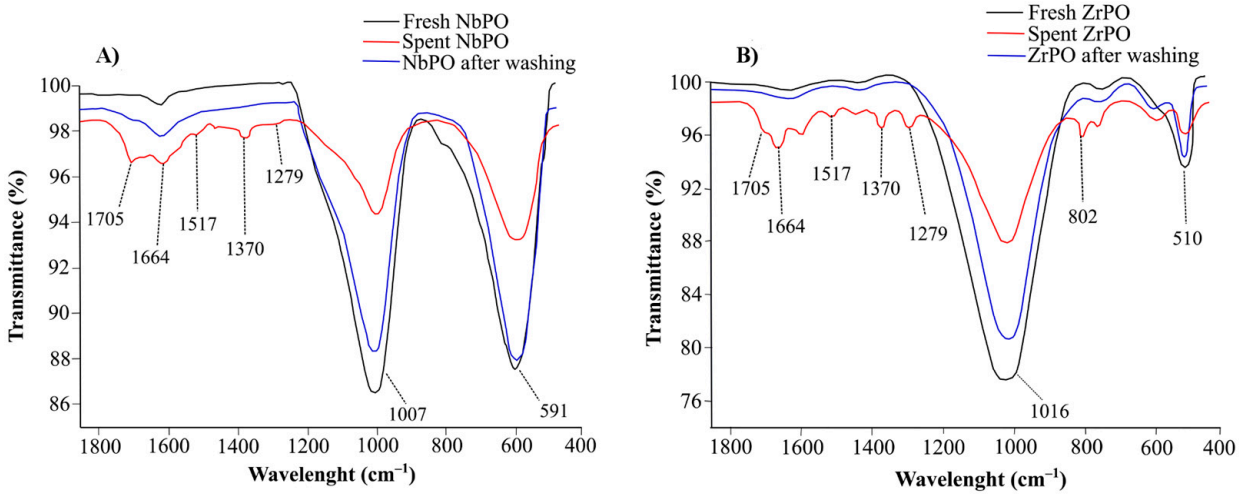

Figure 4. Comparison between FT-IR spectra of fresh NbPO and ZrPO catalysts, spent catalysts and catalysts after washing reactivation in wavenumber range of 1850-430 cm^{-1}: (**A**) NbPO and (**B**) ZrPO.

The spectra of the spent catalysts show characteristic bands of soluble or insoluble humins, proving the deposition of some organic compounds on the catalysts' surface. In fact, absorption bands at 1705 cm^{-1}, 1517 cm^{-1}, 1370 cm^{-1} and 1279 cm^{-1} can be identified both in spent NbPO and ZrPO spectra, and assigned to the stretching of C=O of the carbonyl groups, the stretching of C=C in furan and/or aromatic compounds, the stretching of the C-O-C bond of the furan ring, and the stretching of the C-O bond of the ethers, respectively [2].

In addition, the spectra of the spent NbPO and ZrPO catalysts show another band at 1664 cm^{-1}, due to the stretching of the C=O of the quinones. Moreover, in the spectrum of the spent ZrPO, an additional band at 802 cm^{-1} appears, due to bending out of the plane of the =C-H bond of aromatic and/or furan rings [30]. In Figure 4, the IR spectra of NbPO and ZrPO after the washing treatment are also reported. It is interesting to highlight that the FT-IR spectra of the catalysts after the acetone washing are very similar to those of the fresh samples, thus confirming the feasibility of the proposed simple reactivation method, as indirectly suggested by the recycling tests. The moderate formation of humins during the reaction is also confirmed by SEM analyses, which are reported in Figure 5.

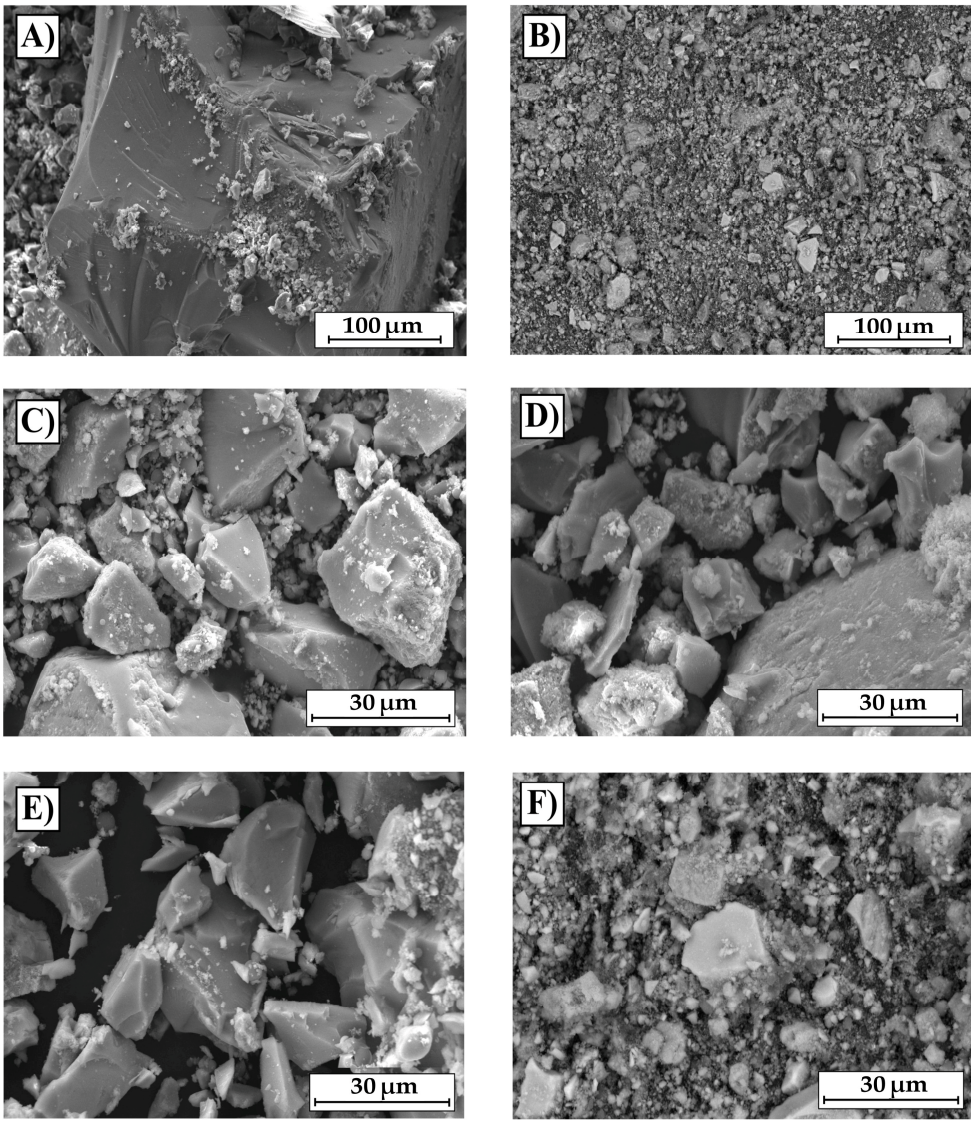

Figure 5. Scanning electron microscopy (SEM): (**A**) fresh NbPO, (**B**) fresh ZrPO, (**C**) spent NbPO, (**D**) spent ZrPO, (**E**) washed NbPO and (**F**) washed ZrPO.

From the SEM of the fresh NbPO and ZrPO, it is possible to see that the morphology of both catalysts reveals pieces and surfaces with irregular dimensions. For the spent catalysts, where NbPO and ZrPO are employed at 160 and 180 °C, respectively (run in Figure 1 after 6 h for NbPO and run in Figure 2 after 6 h for ZrPO), it is possible to observe a few regions covered with particles of spherical morphologies, resulting coalesced each other. Such particles have similar characteristics to insoluble humic compounds, characterized by Patil and Lund [31], confirming the limited formation of these compounds during the

reaction. Figure 5 also shows the washed catalysts, which appear similar to fresh ones, again confirming the feasibility of the washing procedure.

This is also evidenced by TGA analyses on fresh, spent and washed NbPO and ZrPO. The obtained results are shown in Figure 6.

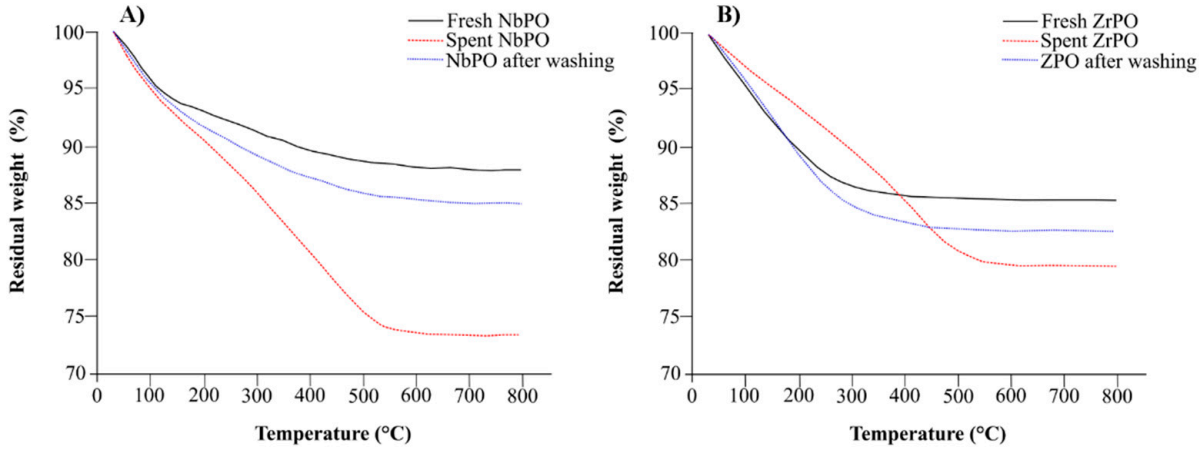

Figure 6. TGA analysis: (**A**) fresh, spent and washed NbPO; (**B**) fresh, spent and washed ZrPO.

The weight loss observed between 30 and 200 °C was due to water and volatile organic compounds (VOCs) [32] trapped in the fresh catalysts. At higher temperatures (between 200 and 500 °C), for the spent NbPO an additional weight loss was observed (about 17 wt%), due to the humins adsorbed on the catalyst surface [32]. On the other hand, for the spent ZrPO, a lower weight loss (about 11 wt%) was ascertained between 200 and 500 °C, thus highlighting a lower amount of adsorbed humins on this catalyst. However, for both catalytic systems, the amount of adsorbed humins is limited and the reactivation treatment performed through acetone washing allowed their removal and the restoration of the starting catalytic activities.

Moreover, the EDS analysis of both phosphates was performed estimating that, on the basis of the elements Nb, Zr and P, the fresh NbPO contained 89.5 wt% niobium and 10.5 wt% phosphorus, whereas the fresh ZrPO was composed of 60.8 wt% zirconium and 39.2 wt% phosphorus. By comparing these results with those of the catalysts after the reactions, it is possible to demonstrate the stability of these phosphates in the adopted reaction conditions: the niobium amount was 89.9 wt% in the spent NbPO system, with a phosphorus amount equal to 10.1 wt%, whereas for the spent ZrPO system, the zirconium amount was 61.4 wt% with 38.6 wt% phosphorus. These results are in agreement with XRF analyses that showed, for the fresh systems, the molar ratios P/Zr and P/Nb were 1.90 ± 0.1 and 0.33 ± 0.05, respectively. On this basis, it is possible to undoubtedly confirm the negligible leaching of Nb and Zr in the aqueous phase under the adopted reaction conditions. This last aspect was also verified by comparing the best catalytic results achieved in the presence of the catalysts (run in Figure 1 for NbPO after 6 h and run in Figure 2 after 6 h for ZrPO) with those obtained after the removal of the catalysts from the reaction medium. For NbPO, after 6 h, the glucose conversion slightly increased, moving from 78.6 to 80.3 mol%, with an almost comparable HMF yield (24.5 mol%). For ZrPO, after 6 h, the same trend was observed, increasing the glucose conversion from 89.0 to 89.9 mol%, together with a similar HMF yield (24.3 mol%).

Finally, the porosities and texture properties of the fresh and spent NbPO and ZrPO systems were analyzed using nitrogen physisorption isotherms, as reported in Figure 7 and Table 7. All samples show type IV isotherms typical of mesoporous materials [33]. In the case of the NbPO samples, very low amounts of microporosities were also present. Noteworthily, both Zr and Nb spent catalysts showed an increase in the hysteresis, due to the formation of ink-bottle pores with a neck size smaller than the average diameter or, in general, due to the presence of pores with diverging radii along their length. This could be

ascribable to the deposition of carbonaceous residue inside the porosities, probably with a greater extent on the external part of the pores. Nonetheless, while NbPO showed a marked decline in both SSA and pore volume, suggesting the occlusion of some of the pores (narrower compared to the ones of ZrPO: 9 nm compared to 16 nm) this was not the case for ZrPO, which is in agreement with the observed catalytic performances and TGA analyses.

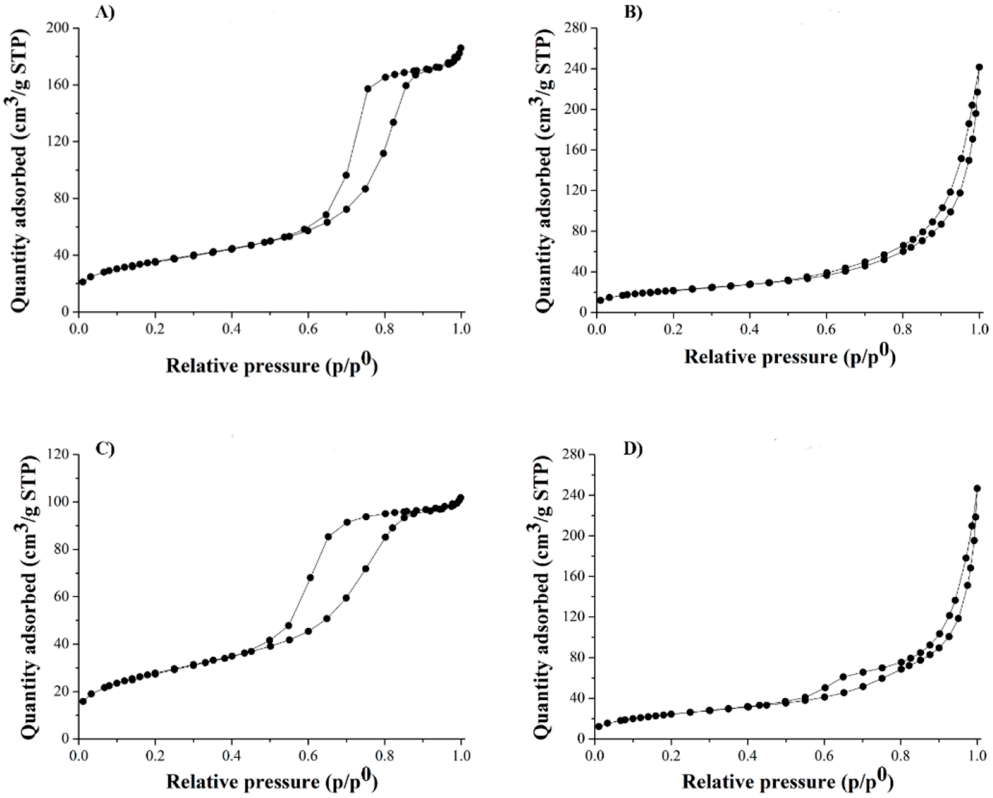

Figure 7. N_2 adsorption and desorption isotherms: (**A**) fresh NbPO, (**B**) fresh ZrPO, (**C**) spent NbPO, (**D**) spent ZrPO.

Table 7. Texture properties of catalysts:fresh NbPO, spent NbPO, fresh ZrPO, spent ZrPO.

Sample	Surface Area (m^2/g)	Total Pore Volume (cm^3/g)	Micropore Volume (cm^3/g)	Micropore Area (m^2/g)	Average Pore Diameter (nm)
Fresh NbPO	133	0.28	0.004	13	9
Fresh ZrPO	108	0.33	0	2	16
Spent NbPO	101	0.16	0.001	6	6
Spent ZrPO	90	0.33	0	0	14

In conclusion, NbPO and ZrPO are characterized by a high stability and an easy recyclability, making them promising for the use with more complex substrates.

2.3. Conversion of Untreated Cellulose in the Presence of NbPO and ZrPO

After the catalytic tests with glucose, the reactivity of the more recalcitrant microcrystalline cellulose was studied in autoclave. Starting from the reaction conditions optimized in a previous work on the conversion of cellulose [34], new catalytic runs were carried out at 150 °C, as in the conversion of glucose in autoclave, and under autogenic pressure, with the same substrate/catalyst weight ratio of 1.2 and cellulose loading of 5 wt%, prolonging the reaction for up to 24 h. The obtained results are reported in Figure 8.

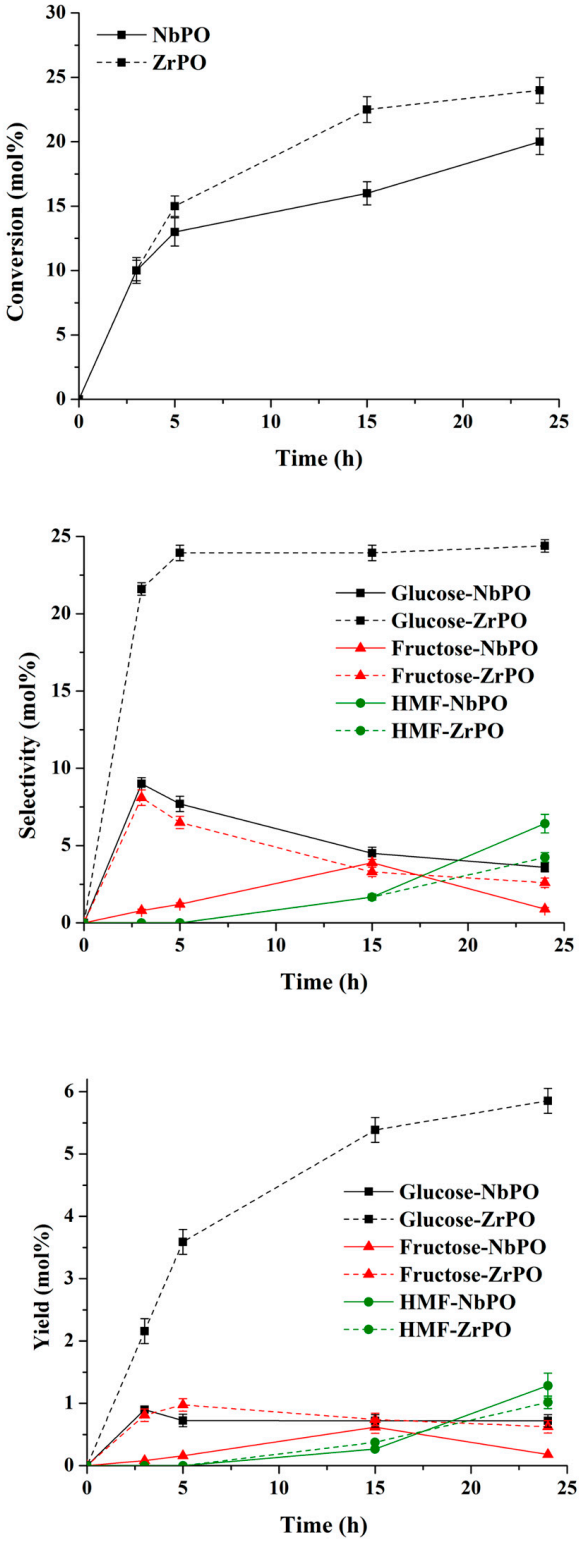

Figure 8. Catalytic performances of NbPO and ZrPO in the conversion of untreated cellulose at 150 °C. Reaction conditions: cellulose = 2.63 g, catalysts = 2.20 g, water = 50.0 g, T = 150 °C, autogenic pressure (LA is present only in traces). Note: where the error bars are not visible, they are smaller than the symbols.

In addition to the reported catalytic runs, a blank test for the conversion of untreated cellulose at 150 °C and 24 h has been performed, obtaining a cellulose conversion of 7 mol%, a glucose yield of 2.3 mol% and only traces of HMF and LA. As it is possible to

appreciate from Figure 8, for both catalytic systems, the cellulose conversion is low, about 20–25 mol%, even though this is higher than that achieved in the blank experiment, with the highest glucose yield of about 6 mol% reached with ZrPO, a value comparable with that reported in the literature adopting ZrPO under analogous reaction conditions (glucose yield 5.8 wt% equal to 5.2 mol%) [34]. It is interesting to note that, starting from cellulose, the higher conversion is achieved with ZrPO, instead of NbPO, as in the case of glucose. This behavior can be justified taking into consideration that starting from cellulose the preliminary hydrolysis step to glucose is necessary and this reaction is mainly catalyzed by Brønsted acidity, but also by Lewis acid sites. In fact, it is known that for efficient cellulose hydrolysis, solid acids must be able to adsorb β-1,4-glucans on the surface and interact with them by means of, for example, acid -OH groups. This interaction can be also promoted by Lewis acid sites [35] and allows a decrease in the activation energy of the hydrolysis step. On this basis, adopting the same amount of NbPO and ZrPO, the ascertained conversion behavior is in agreement with their total acidity, which is higher for ZrPO than NbPO. Regarding the products' distribution, ZrPO shows a higher selectivity towards glucose than NbPO, and this can be justified by the higher amount of total acid sites and the lower Brønsted/Lewis molar ratio of ZrPO, which are responsible for the faster hydrolysis of cellulose to glucose and the slower glucose conversion compared to NbPO, respectively, as previously found. At the same time, the lower Brønsted/Lewis molar ratio of ZrPO than NbPO justifies the higher fructose selectivity observed in ZrPO compared to NbPO. On the other hand, NbPO is more selective towards HMF than ZrPO, in particular in long reaction times, due to the NbPO balanced Brønsted and Lewis acid properties. However, the selectivities of the target products are low for both catalysts (LA is also present only in traces) in the whole investigated time range, suggesting the presence of other not-quantified products, such as oligomers, whose formation is promoted rather than that of glucose due to the limited heterogeneous catalyst interaction with the solid substrate that hampers the hydrolysis step. However, the possibility to obtain hydrolysates rich in cellulose-derived oligomers is very interesting because these are produced under heterogenous catalysis, avoiding any contamination by mineral acids generally employed for their production. Such hydrolysates can be valorized in a plethora of compounds by subsequent catalytic and/or biocatalytic conversion cascade processes, once separated from the solid fraction.

The achieved results employing untreated cellulose are consistent with its nature, in fact it is well known that cellulose is more recalcitrant than glucose towards hydrolysis, due to its stable H-bond networks and high crystalline structure, as confirmed by its XRD analysis (Figure 9), where the main peak at $2\theta = 22.5^\circ$ is attributed to the crystalline fraction. This justifies the lower conversion achieved starting from cellulose.

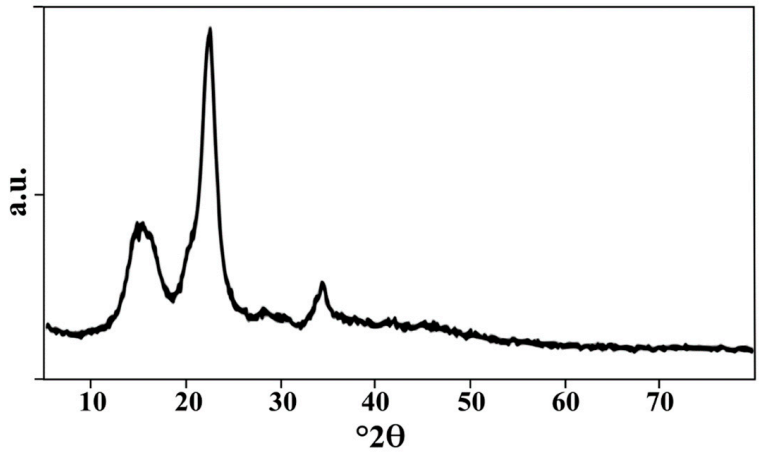

Figure 9. XRD analyses of microcrystalline cellulose.

2.4. Hydrolysis of Real Lignocellulosic Biomasses

On the basis of the promising catalytic performances achieved with NbPO and ZrPO with the model compounds, these systems were also employed with real lignocellulosic biomasses to confirm the correlation between the physical–chemical properties of NbPO and ZrPO and their performances previously identified from the study of model compounds. Conifer wood sawdust was firstly considered as the reference biomass for the hydrolysis tests. Its composition, in terms of cellulose, hemicellulose and lignin, is equal to 45, 20 and 30 wt%, respectively, with 5 wt% of others (extractives, resins and ash). The hydrothermal conversion of conifer wood sawdust into sugars and dehydration/hydrolysis products was investigated in the autoclave, first without any catalyst, and then in the presence of NbPO and ZrPO catalytic systems working at 150 °C with the same substrate/catalyst weight ratio of 1.2 and the biomass loading of 5 wt%. In the absence of a catalyst, the hemicellulose conifer wood sawdust conversion was complete, and the conversion of its cellulose fraction amounted to 7.6 mol%. In addition, the yield to total monosaccharides from hemicellulose was equal to 10.6 mol%, together with traces of monosaccharides from cellulose. In the presence of NbPO and ZrPO, the results are shown in Figure 10.

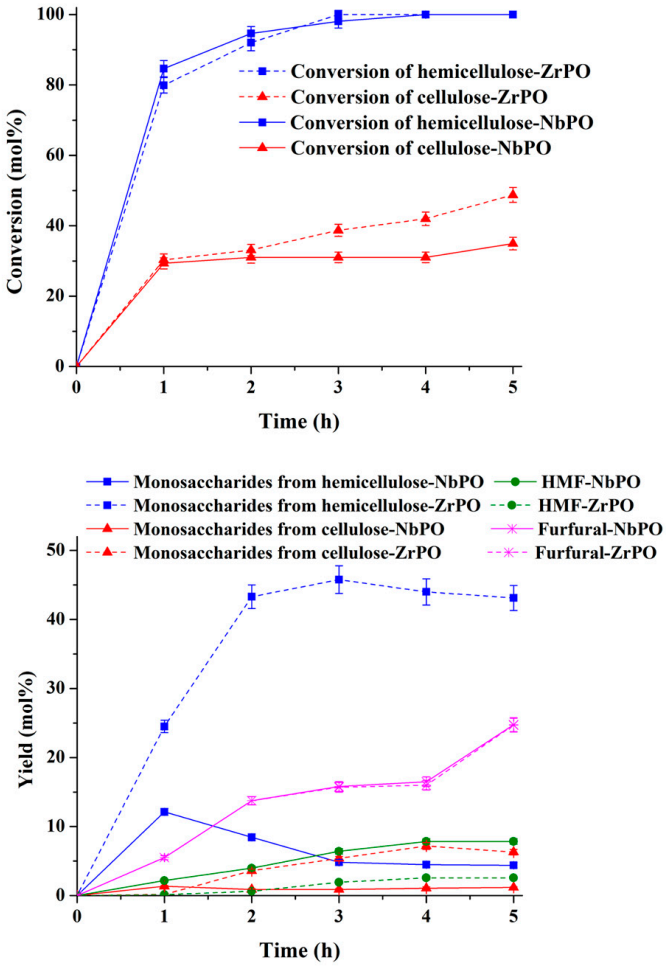

Figure 10. Catalytic performances of NbPO and ZrPO in the conversion of conifer wood sawdust at 150 °C. Reaction conditions: biomass = 2.68 g catalysts = 2.23 g water = 51.0 g T = 150 °C, autogenic pressure. As reported in the Materials and Methods, yields have been calculated with respect to the amount of cellulose or hemicellulose present in the starting biomass. Note: where the error bars are not visible, they are smaller than the symbols.

Noteworthily, for both metal phosphates, the conversion of the hemicellulose fraction of the lignocellulosic substrate is very fast, being almost complete for both systems after

3 h. On the other hand, the conversion of the cellulose fraction is slower, reaching values of 34.9 and 48.8 mol% after 5 h for NbPO and ZrPO, respectively. The observed behavior was expected: hemicellulose hydrolysis proceeds faster and smoother than that of cellulose, as proven by the higher yields of monosaccharides derived from hemicellulose (xylose, arabinose, galactose and mannose) reached when adopting both phosphates. These sugars yields reached the maximum value in a medium–low reaction time, with 45.8 mol% after 3 h for ZrPO and 12.1 mol% after 1 h for NbPO; then, in both cases, these yields decreased due to the increase in decomposition products. Again, the Zr-based catalyst shows higher yield and selectivity towards hemicellulose and cellulose sugars compared with the Nb analogue, while the latter leads to a higher yield and selectivity towards HMF. This behavior is in good agreement with that observed with glucose and cellulose. ZrPO is more active to the degradation of both cellulose and hemicellulose fractions, as shown by the higher achieved cellulose conversion, the most recalcitrant fraction. Conversely, NbPO mainly promotes the formation of furanic derivatives. In fact, the decrease in monosaccharide yield for NbPO begins after only 1 h of reaction time, especially for those deriving from the hemicellulose fraction. This is a much shorter reaction time compared to the 3 h needed with ZrPO. Therefore, it is possible to confirm the effects already found for the hydrolysis of cellulose: the higher total concentration of acid sites, shown by ZrPO, results in a higher activity in lignocellulose conversion and consequently in a higher production of monosaccharides from both hemicellulose and cellulose hydrolysis. On the other hand, the higher amount of strong Brønsted acid sites, exhibited especially in aqueous conditions by NbPO, mainly promotes the dehydration of monosaccharides derived from both cellulose and hemicellulose fractions to successive furan products, such as HMF and furfural. The achieved results are comparable with those reported in the literature by Gliozzi et al., who studied the conversion of conifer wood sawdust in the presence of different acid catalysts [34]. In fact, in the presence of ZrPO, after 5 h of reaction, the authors ascertained at 150 °C the biomass weight conversion of 41 wt%, equal to the 41.9 wt% achieved in the present work (100 mol% of hemicellulose fraction + 48.7 mol% of cellulose fraction), together with the yield of hemicellulose-derived sugars of 49.2 mol% and the yield of cellulose-derived sugars of 3.4 mol%, which are perfectly in agreement with the values ascertained here: 43.1 and 6.3 mol% from hemicellulose and cellulose fractions, respectively.

After having established that the catalytic behavior of Nb and Zr phosphates in hydrolysis reactions is closely related to the catalysts' acid properties in the case of the reference lignocellulosic substrate (conifer wood sawdust), the conversion of a wider range of six real lignocellulosic biomasses was investigated. In particular, Jerusalem artichoke, sorghum, miscanthus, foxtail millet, hemp and *Arundo donax*, whose starting compositions are reported in Table 8, were tested at 150 °C for 1 h in the presence of both Nb and Zr phosphates, adopting the same catalyst/substrate weight ratio of 1.2 and the starting biomass loading of 5 wt%. The results are shown in Tables 9 and 10.

Table 8. Average compositions of the lignocellulosic biomasses employed in the present work.

Biomass	Cellulose (wt%)	Hemicellulose (wt%)	Lignin (wt%)	Others (wt%)
Jerusalem artichoke	16.0	7.5	6.1	70.4
Sorghum	35.7	27.8	6.5	30.0
Miscanthus	23.8	30.9	13.4	31.9
Foxtail millet	16.0	30.9	22.9	30.2
Hemp	62.6	15.1	7.4	14.9
Arundo donax	36.3	24.6	9.4	29.7

Table 9. Catalytic performances of NbPO in the conversion of lignocellulosic biomasses at 150 °C. Reaction conditions: biomass = 2.69 g catalysts = 2.24 g water = 51.0 g T = 150 °C, autogenic pressure, 1 h. As reported in the Materials and Methods, yields have been calculated with respect to the amount of cellulose or hemicellulose present in the starting biomass.

Catalyst: NbPO Biomass	Jerusalem Artichoke	Sorghum	Miscanthus	Foxtail Millet	Hemp	*Arundo donax*
Biomass cellulose conversion (mol%)	76.4	37.8	61.1	73.9	10.7	34.1
Biomass hemicellulose conversion (mol%)	100.0	66.1	66.2	70.2	97.5	69.9
Yield to cellulose-derived sugars (mol%)	19.2	21.9	18.7	24.9	0.6	10.8
Yield to cellulose-derived oligomers (mol%)	23.1	1.7	31.2	29.6	3.1	12.7
Yield to hemicellulose-derived sugars (mol%)	18.8	16.6	25.9	31.2	10.8	20.7
Yield to hemicellulose-derived oligomers (mol%)	34.2	35.1	26.3	26.0	32.6	33.1
Yield to HMF (mol%)	8.6	9.4	5.9	11.7	0.3	5.7
Yield to furfural (mol%)	4.1	2.9	3.7	5.6	2.1	2.9
%C recovered (mol%) respect to starting cellulose amount	74.5	95.2	94.7	92.3	93.3	95.1
%C recovered (mol%) respect to starting hemicellulose amount	57.1	88.5	89.7	92.6	48.0	86.8

Table 10. Catalytic performances of ZrPO in the conversion of lignocellulosic biomasses at 150 °C. Reaction conditions: biomass = 2.67 g catalysts = 2.22 g water = 51.0 g T = 150 °C, autogenic pressure, 1 h. As reported in the Materials and Methods, yields have been calculated with respect to the amount of cellulose or hemicellulose present in the starting biomass.

Catalyst: ZrPO Biomass	Jerusalem Artichoke	Sorghum	Miscanthus	Foxtail Millet	Hemp	*Arundo donax*
Biomass cellulose conversion (mol%)	97.7	49.9	78.2	85.5	14.9	41.4
Biomass hemicellulose conversion (mol%)	100.0	74.2	76.7	76.5	100.0	65.0
Yield to cellulose-derived sugars (mol%)	50.0	31.0	25.0	35.5	2.3	14.2
Yield to cellulose-derived oligomers (mol%)	28.4	5.2	48.0	44.9	3.1	21.4
Yield to hemicellulose-derived sugars (mol%)	21.0	19.5	24.6	34.7	10.2	20.6
Yield to hemicellulose-derivedoligomers (mol%)	34.4	34.6	26.5	26.2	41.3	33.2
Yield to HMF (mol%)	4.5	5.9	3.7	5.1	1.5	2.4
Yield to furfural (mol%)	1.9	1.4	1.5	2.3	2.1	1.9
%C recovered (mol%) respect to starting cellulose amount	85.2	92.2	98.5	100.0	92.0	96.6
%C recovered (mol%) respect to starting hemicellulose amount	57.3	81.3	75.9	86.7	53.6	90.7

The results show that the catalytic performances are significantly affected by the composition of the substrates. For both catalysts and for most biomasses (except for foxtail millet with ZrPO), the conversion of hemicellulose is higher or comparable to that of cellulose, and this is in agreement with the easier hydrolysis of the C5 fraction than the C6 one. In particular, the percentage of the hardly hydrolyzable cellulose present in the starting biomass compared with the hemicellulose amount influences the biomass conversion: in fact, hemp, which is characterized by a cellulose content of 62.6 wt%, shows the lowest cellulose conversion with both phosphates, 10.7 and 14.9 mol% for NbPO and ZrPO, whereas Jerusalem artichoke reveals the highest conversions of cellulose, equal to 76.4 and 97.7 mol% for NbPO and ZrPO, due to the lower cellulose percentage of only 16.0 wt%. Regarding the products' yields, the achieved results employing the six agricultural waste substrates are in good accordance with those obtained from glucose and cellulose, but also from the reference biomass conifer wood sawdust: ZrPO shows a higher selectivity than NbPO towards cellulose-derived sugars and cellulose-derived oligomers, whereas the behavior towards hemicellulose-derived sugars and hemicellulose-derived oligomers is similar for the two catalysts. The possibility of obtaining such hydrolysates rich in hemicellulose- and cellulose-derived sugars/oligomers, in particular those prepared by Jerusalem artichoke, miscanthus and foxtail millet with NbPO and ZrPO, characterized by a high hemicellulose and cellulose solubilization, opens the possibility for many subsequent catalytic and/or biocatalytic cascade processes towards the production of several compounds. Moreover, the employment of heterogeneous catalysts allows avoiding any contamination once the solid residue is separated, as happens with mineral acids generally employed for this reaction [36,37]. From the perspective of developing such a cascade process, the recovered solid residue could be exploited by many strategies, according to the sustainability criteria. In fact, the final solid residue is a hydrochar, more similar to lignin than to the starting lignocellulosic biomasses and, as such, it could be used in energy and environmental fields, including applications as adsorbents, precursors of catalysts, soil amendment, anaerobic digestion, composting and electrochemical energy storage materials [38].

Moreover, as previously stated, NbPO shows a prevailing performance towards sugar consecutive products, such as HMF and furfural, whose yield for NbPO are higher with respect to those observed for ZrPO. With respect to conifer wood sawdust, after 1 h of reaction, Jerusalem artichoke biomass shows a higher cellulose conversion with both phosphates than conifer wood sawdust (97.7 mol% with ZrPO and 76.4 mol% with NbPO for Jerusalem artichoke, with respect to 30.3 mol% with ZrPO and 29.3 mol% with NbPO for conifer wood sawdust). The higher conversion achieved for Jerusalem artichoke rather than conifer wood sawdust is also observed for its hemicellulose fraction after 1 h of reaction with both catalysts (100.0 mol% with ZrPO and NbPO for Jerusalem artichoke, with respect to 79.9 mol% with ZrPO and 84.6 mol% with NbPO for conifer wood sawdust). In addition, the yields of monosaccharides derived from cellulose with both phosphates are also higher than the corresponding ones achieved with conifer wood sawdust. In fact, the yields of cellulose-derived sugars equal to 50.0 and 19.2 mol% with ZrPO and NbPO, obtained starting from Jerusalem artichoke, were higher than those ascertained from conifer wood sawdust (0.2 and 1.4 mol% with ZrPO and NbPO, respectively). Regarding yields to hemicellulose-derived sugars, it is possible to underline that after 1 h of reaction in the presence of ZrPO, comparable values were reached with Jerusalem artichoke and conifer wood sawdust (21.0 mol% for Jerusalem artichoke and 24.5 mol% for conifer wood sawdust), whereas under the same reaction conditions in the presence of NbPO, a higher yield of hemicellulose-derived sugars was obtained starting from Jerusalem artichoke (18.8 mol%) compared with conifer wood sawdust (12.1 mol%). Moreover, taking into consideration the yield of furanic compounds (HMF + furfural), the achieved yields starting from Jerusalem artichoke are higher than those obtained from conifer wood sawdust (6.4 mol% with ZrPO and 12.7 mol% with NbPO for Jerusalem artichoke, with respect to 5.6 mol% with ZrPO and 7.7 mol% with NbPO for conifer wood sawdust). The achieved results highlight that

Jerusalem artichoke is a promising biomass to produce furanic compounds and cellulose-derived sugars after only 1 h of reaction in the presence of NbPO and ZrPO, respectively.

In the literature, the use of metal phosphates to produce HMF from real biomasses is rare, and the substrates are mostly limited to monosaccharides [1]. From this perspective, Parshetti et al. investigated the conversion of food waste biomass to HMF, reaching, under the best reaction condition, an HMF yield of 4.3 wt% in the presence of ZrPO calcinated at 400 °C after 6 h of reaction [27]. This value is comparable with those reached in the present work after only 1 h of reaction starting from Jerusalem artichoke (1.1 wt%), sorghum (2.6 wt%), miscanthus (1.1 wt%), foxtail millet (1.5 wt%) and *Arundo donax* (1.6 wt%) in the presence of NbPO, starting from sorghum (1.6 wt%) in the presence of ZrPO. Finally, in all runs reported in Tables 9 and 10, the %C recovered (mol%) value underlines the moderate presence of humins, which is higher for NbPO than ZrPO.

In conclusion, starting from raw lignocellulosic biomasses, NbPO and ZrPO enable us to achieve high percentages of hemicellulose and cellulose solubilization and hydrolysates rich in hemicellulose and cellulose sugars and oligomers to be further valorized. In particular, starting from Jerusalem artichoke, in the presence of NbPO and ZrPO, yields of furanic compounds of 12.7 mol% and cellulose-derived sugars of 50.0 mol% were achieved after only 1 h of reaction, respectively, thus confirming their high potential as heterogeneous acid catalysts in biomass conversion.

As previously reported, NbPO and ZrPO showed high stability and easy recyclability when employed in the glucose conversion. However, in order to demonstrate the real feasibility of their employment in the conversion of real feedstocks, their recyclability was further investigated, in particular for Jerusalem artichoke, the most promising biomass. In this case, the solids recovered at the end of the catalytic reactions contained not only the spent catalyst, but also the unconverted biomass, thus making the separation of the catalyst from the substrate and its recycling more complex. For this purpose, the solid residues recovered from the hydrolysis of Jerusalem artichoke with NbPO and ZrPO were thermally treated at 500 °C for 5 h with the aim of burning the unconverted biomass and recovering the catalysts, which are stable at this temperature, as demonstrated by the TGA (Figure 6). The post-treated NbPO and ZrPO catalysts were subsequently employed within two other recycling runs under the same reaction conditions of the first one (150 °C, autogenic pressure, 1 h). Regarding the conversion of the Jerusalem artichoke hemicellulose fraction, both recycled catalysts gave analogous results in the first run (results are not shown), whereas some differences were observed in the conversion of the cellulose fraction, as shown in Figure 11.

The results further confirmed that the hydrolysis of hemicellulose was easier than that of cellulose and an irrelevant deactivation of the catalysts during their recycle did not affect conversion. On the other hand, the slight deactivation of both catalysts caused a small decrease in cellulose conversion, together with a decrease in HMF and sugar yields and an increase in oligomer yields, as the hydrolysis of cellulose is partly limited by the slight loss of catalytic activity. In particular, after the third recycling run of NbPO, the cellulose conversion, sugar yield and HMF yield decreased from 76.4, 19.2 and 8.6 mol% to 68.3, 14.1 and 2.5 mol%, respectively, in favor of the oligomer formation that achieved the yield of 30.3 mol% from 23.1 mol% (Figure 11A). Regarding ZrPO, after the third recycle run, the cellulose conversion moderately decreased to 94.4 mol% from 97.7 mol%, analogously to sugars and HMF yields that lowered from 50.0 and 4.5 mol% to 43.1 and 1.8 mol%, respectively, whereas the oligomer yield raised to 35.4 mol% from 28.4 mol% (Figure 11B). In conclusion, the thermal treatment of the solid residues, recovered at the end of the process, represents an efficient strategy for the removal of unconverted biomass and allows the successful recycle of catalysts that maintain almost unchanged their starting catalytic activity.

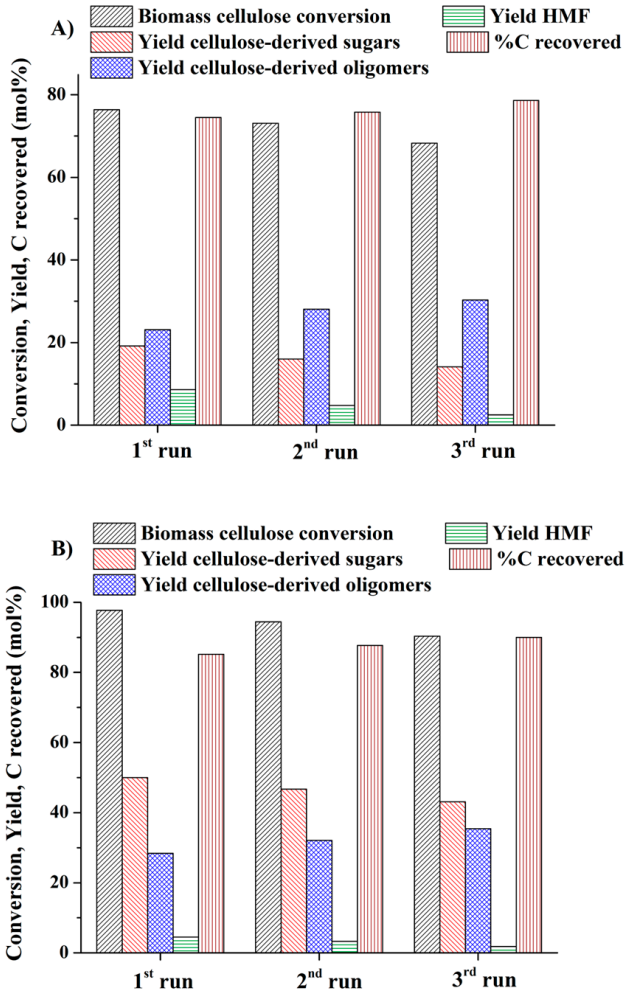

Figure 11. Conversion of Jerusalem artichoke cellulosic fraction in the recycle runs of: (**A**) NbPO and (**B**) ZrPO at 150 °C. Reaction conditions: biomass = 2.68 g catalysts = 2.23 g water = 51.0 g T = 150 °C, autogenic pressure, 1 h. As reported in the Materials and Methods, yields have been calculated with respect to the amount of cellulose or hemicellulose present in the starting biomass.

3. Materials and Methods

3.1. Materials

Glucose, xylose, fructose, LA and furfural were purchased from Sigma-Aldrich (Sigma-Aldrich, St. Louis, MO, USA) and used as received. HMF was supplied by AVA Biochem (AVA Biochem AG, Zug, Switzerland). NbPO was kindly provided by CBMM (Companhia Brasileira de Metalurgia e Mineracão, Araxá, Minas Gerais, Brasil). It was calcined in static air at 400 °C for 3 h with a heating rate of 10°C/min before its use. ZrPO was prepared according to the procedure reported by Kamiya et al. [39]. In particular, two different solutions were prepared in two different beakers by dissolving 10.5 g of $ZrOCl_2 \cdot 8H_2O$ in 32 mL of distilled water (1 M) and 7.4 g of $NH_4H_2PO_4$ in 64 mL of water (1 M). The latter solution was added dropwise, under magnetic stirring (600 rpm), to the first beaker at room temperature without any other expedients, obtaining the precipitation of a white solid characterized by a P/Zr atomic ratio equal to 2. The precipitate was then filtered, washed with distilled water, dried at 100 °C and finally calcined in static air at 400 °C for 3 h with a heating rate of 10 °C/min before its use. Microcrystalline cellulose Avicel PH-101 (particle size 50 µm) was purchased from Sigma-Aldrich (Sigma-Aldrich, St. Louis, MO, USA) and used as received, whereas the ball-milled sample was achieved after treatment in a tungsten carbide vial for 48 h. Lignocellulosic waste biomasses, namely, conifer wood sawdust, Jerusalem artichoke, sorghum, miscanthus, foxtail millet, hemp and *Arundo donax*,

were provided by Prof. Monti and Prof. Zanetti of the Agriculture School of the University of Bologna. All biomasses were dried and ball-milled for 15 min before the catalytic tests.

3.2. Catalytic Reactions

The conversion tests of glucose, cellulose and real lignocellulosic biomasses (conifer wood sawdust, Jerusalem artichoke, sorghum, miscanthus, foxtail millet, hemp and *Arundo donax*) were performed in an autoclave, adopting a 300 mL mechanically stirred Parr 4560 reactor (Parr Instrument Company, Moline, IL, USA) equipped with a P.I.D. controller 4843, an electrical heating system, and temperature and stirring control devices. In a typical procedure, the desired amounts of the catalyst, substrate and water were placed in the reactor, which was then subjected to repeated cycles of evacuation and nitrogen flushing to ensure complete oxygen removal. Isothermal conditions were maintained for the desired reaction time. In each experiment, time zero was taken as the beginning of the isothermal stage. Reaction mixture samples were periodically withdrawn through the sampling valve during the reaction, quickly cooled and analyzed by HPLC. At the end of the reaction, the mixture was cooled, collected in water and then filtered over a Buchner filter. After the filtration, the solid residue was recovered, dried overnight at 80 °C in an oven, and then analyzed to determine the conversion of the biomass substrate. Each test was performed in triplicate.

Glucose conversion reactions were also performed in a monomodal microwave reactor CEM Discover S-class System (CEM Corporation, Matthews, NC, USA). In a standard reaction, the feedstock was charged in the microwave (MW) reactor (10 mL) with the proper amount of the catalyst. The vessel was placed in the chamber of the MW reactor and heated up to reach the desired temperature for the selected time under magnetic stirring. At the end of the reaction, the vessel was cooled at room temperature through an external air flow that allows fast cooling, and a portion of the sample was taken for the analysis. Each test was performed in triplicate.

HPLC analyses were carried out using an Agilent 1260 Infinity Series HPLC system (Agilent Technologies, Santa Clara, CA, USA) equipped with a manual injector with a 20 µL calibrated loop equipped with two different columns. The quantification of monosaccharides was performed by using an Agilent Hi-Plex Pb column (Agilent Technologies, Santa Clara, CA, USA) (length = 30 cm, diameter = 7.7 mm, particle size = 8 µm) whose stationary phase was made of a divinylbenzene–styrene copolymer functionalized with Pb^{2+} ions. The column was thermostated at 80 °C and 0.6 mL/min flow of water was used as eluent. The detection of products occurred by means of a refraction index detector (RID), thermostated at 40 °C. On the other hand, the quantification of organic acids and furans was carried out by adopting a Phenomenex Rezex ROA-H column (Phenomenex, Torrance, CA, USA) (length = 30 cm, diameter = 7.7 mm, particle size = 8 µm) whose stationary phase was made of a divinylbenzene–styrene copolymer functionalized with H^+ ions. The column was thermostated at 60 °C and 0.6 mL/min flow of 0.0025 M H_2SO4 solution was used as eluent. The detection of products occurred by means of a UV–diode array detector (UV-DAD), recording the absorbance at 253, 205 and 192 nm.

The oligomer quantification and the analysis of the chemical composition of both starting raw biomasses and treated residues were evaluated following the standard procedure of Sluiter et al. [40].

The catalytic performances were reported in terms of conversion, selectivity and yield. These last were calculated on a molar basis, considering glucose or the anhydroglucose unit of cellulose. In the following equations, glucose is always reported as a reference.

Glucose conversion (mol%) = [(moles glucose in − moles glucose out)/moles glucose in] × 100;

Selectivity to compound i (mol%) = [(moles compound i)/(moles glucose in − moles glucose out)] × 100;

Yield to compound i (mol%) = (moles compound i/moles glucose in) × 100.

For lignocellulosic biomasses, catalytic performances were also expressed in terms of molar basis, adopting the Sluiter protocol for the quantification of oligomers [40]. In particular, the conversion of cellulose and hemicellulose, the yields of sugars (glucose and fructose) and oligomers coming from cellulose, the yields of sugars (xylose, arabinose, galactose and mannose) and oligomers coming from hemicellulose, the HMF yield (deriving from cellulose) and the furfural yield (deriving from hemicellulose) were considered and calculated according to the following equations.

Biomass cellulose conversion (mol%) = [(moles anhydroglucose cellulose in − moles anhydroglucose residue out)/moles anhydroglucose cellulose in] × 100;

Biomass hemicellulose conversion (mol%) = [(moles anhydroxylose hemicellulose in – moles anhydroxylose residue out)/moles anhydroxylose hemicellulose in] × 100;

Cellulose-derived sugars yield (mol%) = [(moles glucose + moles fructose)/(moles anhydroglucose cellulose in)] × 100;

Cellulose-derived oligomers yield (mol%) = [(moles glucose out post Sluiter − moles glucose out post reaction)/moles anhydroglucose cellulose in] × 100;

Hemicellulose-derived sugars yield (mol%) = [(moles xylose + moles arabinose + moles galactose + moles mannose)/(moles anhydroxylose hemicellulose in)] × 100;

Hemicellulose-derived oligomers yield (mol%) = [(moles xylose out post Sluiter − moles xylose out post reaction)/moles anhydroxylose hemicellulose in] × 100;

HMF yield (mol%) = [(moles HMF)/(moles anhydroglucose cellulose in)] × 100;

Furfural yield (mol%) = [(moles furfural)/(moles anhydroxylose hemicellulose in)] × 100.

The %C recovered was evaluated as the sum of the moles of products and moles of unconverted reagent (glucose and/or anhydrosugars for cellulose and real biomasses) with respect to the initial moles of the reagent (glucose and/or anhydrosugars for cellulose and real biomasses) and expressed in mol%.

All the experiments were carried out in triplicate and the reproducibility of the technique was within 5%.

The catalysts employed in the conversion of Jerusalem artichoke were separated from the unconverted biomass through the thermal treatment that allowed the combustion of the organic matter. This thermal treatment was performed in a muffle furnace Nabertherm L 9/11/SKM/P330 (Nabertherm, Lilienthal, Germany) at 500 °C for 5 h.

3.3. Analysis of Catalyst Properties

The main characterization of fresh NbPO and ZrPO was reported in our previous work [2].

XRD analyses were carried out using a vertical goniometer diffractometer: Philips PW 1050/81 (Philips, Amsterdam, The Netherlands). The analyses were performed using CuK radiation, which was made monochromatic by using a nickel filter with $\lambda = 0.15418$ nm. The adopted interval was $5^\circ < 2\theta < 80^\circ$, with steps of 0.2°; the count of intensity was carried out every 2 s.

FT-IR analyses were recorded in ATR mode with a Spectrum Two Perkin Elmer FT-IR spectrometer (Perkin Elmer, Waltham, MA, USA) in the range of wavenumber 4000-450 cm^{-1}.

TGA analyses were performed by using a TGA Q500 instrument (TA Instruments, New Castle, DE, USA) in the temperature range of 30–800 °C at a heating rate of 10 °C/min and under an air flow of 20 mL/min.

Scanning electron microscopy associated with energy-dispersion spectrometry (SEM/EDS) analysis was performed with a JEOL -6010/LA microscope (JEOL Ltd., Tokyo, Japan). The EDS spectra were obtained using a working distance of 10 mm and a voltage of 20 KV. The crystal structure of the catalyst was evaluated by a Bruker model D8 X-ray diffractometer (Bruker, Billerica, MA, USA) discovered under Cu Kα ($\lambda = 0.15441$ nm) in the 2θ range of 5–80° at a scan rate of 3°/min.

XRF analyses were performed by employing a wavelength dispersive spectrometer Panalytical Axios Advanced (Malvern Panalytical, Malvern, UK) equipped with tube rhodium and characterized by a power of 4 kW.

Nitrogen adsorption/desorption isotherms (77 K) were recorded at −196 °C using a Micromeritics ASAP 2020 instrument (Micromeritics, Norcross, GA, USA). Samples were previously outgassed for 120 min at 423 K and 30 μmHg and then heated for 240 min at 623 K. Specific surface area values were obtained by using the multi-point BET equation in the 0.05–0.2 p/p0 range and total pore volume values were calculated at 0.95 p/p0.

4. Conclusions

In this work, niobium and zirconium phosphates were tested as heterogeneous acid catalysts for the hydrothermal conversion of glucose, cellulose and six strategic lignocellulosic biomasses produced as agricultural and forestry residues, such as conifer wood sawdust, Jerusalem artichoke, sorghum, miscanthus, foxtail millet, hemp and *Arundo donax*. Among the available heterogeneous acid catalysts, the metal phosphates were very promising due to their high thermal stability and good water tolerance. The HMF yield of 24.4 mol% and the LA yield of 24.0 mol% were achieved starting from model compounds using niobium and zirconium phosphates at 160 and 180 °C, respectively. On the other hand, when real lignocellulosic biomasses were employed as the substrate, both catalysts fostered hemicellulose and cellulose solubilization. In particular, starting from the Jerusalem artichoke, miscanthus and foxtail millet, hydrolyzates rich in C5 and C6 sugars and oligomers were produced. These hydrolyzates can be further valorized towards production in a wide range of bio-based compounds through catalytic and/or biocatalytic conversion cascade processes. Zirconium phosphate promoted the hydrolysis of the starting biomasses, causing a higher production of monosaccharides from cellulose and hemicellulose, such as glucose and fructose from the cellulose fraction, and xylose, arabinose, galactose and mannose from the hemicellulose one. Differently, niobium phosphate was active towards the sugars' consecutive products derived from C5 and C6, such as furfural and HMF. In particular, starting from the Jerusalem artichoke, the yield of furanic compounds was 12.7 mol%, while the yield of cellulose-derived sugars was 50.0 mol% in the presence of niobium and zirconium phosphate, respectively, after only 1 h of reaction, adopting the biomass/catalyst weight ratio of 1.2, thus resulting a promising starting feedstock for moving towards heterogeneously catalyzed biomass conversion. These behaviors were related to the acid properties of the proposed catalysts, in particular, the total acidity, the Brønsted/Lewis acid sites ratio and their strength, giving us the opportunity to better tune the reaction towards the target products.

Author Contributions: Conceptualization, C.A., A.M.R.G. and F.C.; methodology, C.A., A.M.R.G., A.M. and F.C.; formal analysis, C.A., D.L., S.F., N.D.F., F.Z. and T.T.; writing—original draft preparation, C.A., D.L. and T.T.; writing—review and editing, C.A., A.M.R.G., A.M. and F.C.; supervision, C.A., A.M.R.G. and F.C. All authors have read and agreed to the published version of the manuscript.

Funding: This research received no external funding.

Acknowledgments: The authors are grateful to Italian Ministero dell'Università e della Ricerca for the financial support provided through the PRIN 2020 LEVANTE project "LEvulinic acid Valorization through Advanced Novel Technologies" (Progetti di Ricerca di Rilevante Interesse Nazionale-Bando 2020, 2020CZCJN7).

Conflicts of Interest: The authors declare no conflict of interest.

References

1. Xu, H.; Li, X.; Hu, W.; Lu, L.; Chen, J.; Zhu, Y.; Zhou, H.; Si, C. Recent advances on solid acid catalytic systems for production of 5-hydroxymethylfurfural from biomass derivatives. *Fuel Process. Technol.* **2022**, *234*, 107338–107356. [CrossRef]
2. Antonetti, C.; Melloni, M.; Licursi, D.; Fulignati, S.; Ribechini, E.; Rivas, S.; Parajó, J.C.; Cavani, F.; Raspolli Galletti, A.M. Microwave-assisted dehydration of fructose and inulin to HMF catalyzed by niobium and zirconium phosphate catalysts. *Appl. Catal. B Environ.* **2017**, *206*, 364–377. [CrossRef]

3. Azlan, N.S.M.; Yap, C.L.; Gan, S.; Rahman, M.B.A. Recent advances in the conversion of lignocellulosic biomass and its degraded products to levulinic acid: A synergy of Brønsted-Lowry acid and Lewis acid. *Ind. Crops Prod.* **2022**, *181*, 114778–114802. [CrossRef]
4. Antonetti, C.; Licursi, D.; Fulignati, S.; Valentini, G.; Raspolli Galletti, A.M. New frontiers in the catalytic synthesis of levulinic acid: From sugars to raw and waste biomass as starting feedstock. *Catalysts* **2016**, *6*, 196. [CrossRef]
5. Messori, A.; Fasolini, A.; Mazzoni, R. Advances in Catalytic Routes for the homogeneous green conversion of the bio-based platform 5-hydroxymethylfurfural. *ChemSusChem* **2022**, *15*, 202200228–202200245. [CrossRef]
6. Rivas, S.; Raspolli Galletti, A.M.; Antonetti, C.; Licursi, D.; Santos, V.; Parajó, J.C. A biorefinery cascade conversion of hemicellulose-free *Eucalyptus globulus* wood: Production of concentrated levulinic acid solutions for γ-valerolactone sustainable preparation. *Catalysts* **2018**, *8*, 169. [CrossRef]
7. Fulignati, S.; Antonetti, C.; Wilbers, E.; Licursi, D.; Heeres, H.J.; Raspolli Galletti, A.M. Tunable HMF hydrogenation to furan diols in a flow reactor using Ru/C as catalyst. *J. Ind. Eng. Chem.* **2021**, *100*, 390.e1–390.e9. [CrossRef]
8. Xu, W.P.; Chen, X.F.; Guo, H.J.; Li, H.L.; Zhang, H.R.; Xiong, L.; Chen, X.D. Biotechnology. Conversion of levulinic acid to valuable chemicals: A review. *J. Chem. Technol. Biotechnol.* **2021**, *96*, 3009–3024. [CrossRef]
9. Shi, N.; Liu, Q.; Cen, H.; Ju, R.; He, X.; Ma, L. Formation of humins during degradation of carbohydrates and furfural derivatives in various solvents. *Biomass Convers. Biorefinery* **2020**, *10*, 277–287. [CrossRef]
10. Shi, N.; Liu, Q.; Ju, R.; He, X.; Zhang, Y.; Tang, S.; Ma, L. Condensation of α-carbonyl aldehydes leads to the formation of solid humins during the hydrothermal degradation of carbohydrates. *ACS Omega* **2019**, *4*, 7330–7343. [CrossRef]
11. Deng, L.; Li, J.; Lai, D.M.; Fu, Y.; Guo, Q.X. Catalytic conversion of biomass-derived carbohydrates into γ-valerolactone without using an external H_2 supply. *Angew. Chem. Int. Ed.* **2009**, *121*, 6651–6654. [CrossRef]
12. Flannelly, T.; Lopes, M.; Kupiainen, L.; Dooley, S.; Leahy, J. Non-stoichiometric formation of formic and levulinic acids from the hydrolysis of biomass derived hexose carbohydrates. *RSC Adv.* **2016**, *6*, 5797–5804. [CrossRef]
13. Acharjee, T.C.; Lee, Y.Y. Production of levulinic acid from glucose by dual solid-acid catalysts. *Environ. Prog. Sustain. Energy* **2018**, *37*, 471–480. [CrossRef]
14. Weingarten, R.; Kim, Y.T.; Tompsett, G.A.; Fernández, A.; Han, K.S.; Hagaman, E.W.; Conner Jr, W.C.; Dumesic, J.A.; Huber, G.W. Conversion of glucose into levulinic acid with solid metal (IV) phosphate catalysts. *J. Catal.* **2013**, *304*, 123–134. [CrossRef]
15. Marianou, A.A.; Michailof, C.M.; Pineda, A.; Iliopoulou, E.; Triantafyllidis, K.; Lappas, A. Effect of Lewis and Brønsted acidity on glucose conversion to 5-HMF and lactic acid in aqueous and organic media. *Appl. Catal. A: Gen.* **2018**, *555*, 75–87. [CrossRef]
16. Wang, K.; Liang, C.; Zhang, Q.; Zhang, F. Synergistic catalysis of Brønsted acid and Lewis acid coexisted on ordered mesoporous resin for one-pot conversion of glucose to 5-hydroxymethylfurfural. *ACS Omega* **2019**, *4*, 1053–1059. [CrossRef]
17. Krawielitzki, S. AVA Biochem, Pioneer in industrial biobased furan chemistry. *Chimia* **2020**, *74*, 776–778. [CrossRef] [PubMed]
18. Hu, D.; Zhang, M.; Xu, H.; Wang, Y.; Yan, K. Recent advance on the catalytic system for efficient production of biomass-derived 5-hydroxymethylfurfural. *Renewable and Sustainable Energy Reviews* **2021**, *147*, 111253. [CrossRef]
19. Villa, A.; Schiavoni, M.; Fulvio, P.F.; Mahurin, S.M.; Dai, S.; Mayes, R.T.; Veith, G.M.; Prati, L. Phosphorylated mesoporous carbon as effective catalyst for the selective fructose dehydration to HMF. *J. Energy Chem.* **2013**, *22*, 305–311. [CrossRef]
20. Van der Graaf, W.N.P.; Tempelman, C.H.L.; Hendriks, F.C.; Ruiz-Martinez, J.; Bals, S.; Weckhuysen, B.M.; Pidko, E.A.; Hensen, E.J.M. Deactivation of Sn-Beta during carbohydrate conversion. *Appl. Catal. A Gen.* **2018**, *564*, 113–122. [CrossRef]
21. Oozeerally, R.; Burnett, D.L.; Chamberlain, T.W.; Kashtiban, R.J.; Huband, S.; Walton, R.I.; Degirmenci, V. Systematic modification of UiO-66 metal-organic frameworks for glucose conversion into 5-hydroxymethyl furfural in water. *ChemCatChem* **2021**, *13*, 2517–2529. [CrossRef]
22. Zhang, Y.; Wang, J.; Li, X.; Liu, X.; Xia, Y.; Hu, B.; Lu, G.; Wang, Y. Direct conversion of biomass-derived carbohydrates to 5-hydroxymethylfurural over water-tolerant niobium-based catalysts. *Fuel* **2015**, *139*, 301–307. [CrossRef]
23. De Jesus Junior, M.M.; Fernandes, S.A.; Borges, E.; Baêta, B.E.L.; De Ávila Rodrigues, F. Kinetic study of the conversion of glucose to 5-hydroxymethylfurfural using niobium phosphate. *Mol. Catal.* **2022**, *518*, 112079–112088. [CrossRef]
24. Ordomsky, V.; Sushkevich, V.; Schouten, J.; Van Der Schaaf, J.; Nijhuis, T. Glucose dehydration to 5-hydroxymethylfurfural over phosphate catalysts. *J. Catal.* **2013**, *300*, 37–46. [CrossRef]
25. Liu, Q.; Liu, H.; Gao, D.M. Establishing a kinetic model of biomass-derived disaccharide hydrolysis over solid acid: A case study on hierarchically porous niobium phosphate. *Chem. Eng. J.* **2022**, *430*, 132756–132765. [CrossRef]
26. Saravanan, K.; Park, K.S.; Jeon, S.; Bae, J.W. Aqueous phase synthesis of 5-hydroxymethylfurfural from glucose over large pore mesoporous zirconium phosphates: Effect of calcination temperature. *ACS Omega* **2018**, *3*, 808–820. [CrossRef]
27. Parshetti, G.K.; Suryadharma, M.S.; Pham, T.P.T.; Mahmood, R.; Balasubramanian, R. Heterogeneous catalyst-assisted thermochemical conversion of food waste biomass into 5-hydroxymethylfurfural. *Bioresour. Technol.* **2015**, *178*, 19–27. [CrossRef] [PubMed]
28. Vieira, J.L.; Paul, G.; Iga, G.D.; Cabral, N.M.; Bueno, J.M.C.; Bisio, C.; Gallo, J.M.R. Niobium phosphates as bifunctional catalysts for the conversion of biomass-derived monosaccharides. *Appl. Catal. A Gen.* **2021**, *617*, 118099–118109. [CrossRef]
29. Antonetti, C.; Gori, S.; Licursi, D.; Pasini, G.; Frigo, S.; López, M.; Parajó, J.C.; Raspolli Galletti, A.M. One-pot alcoholysis of the lignocellulosic *Eucalyptus nitens* biomass to *n*-butyl levulinate, a valuable additive for diesel motor fuel. *Catalysts* **2020**, *10*, 509. [CrossRef]

30. Tatzber, M.; Stemmer, M.; Spiegel, H.; Katzlberger, C.; Haberhauer, G.; Mentler, A.; Gerzabek, M.H. FTIR-spectroscopic characterization of humic acids and humin fractions obtained by advanced NaOH, $Na_4P_2O_7$, and Na_2CO_3 extraction procedures. *J. Plant Nutr. Soil Sci.* **2007**, *170*, 522–529. [CrossRef]
31. Patil, S.K.; Lund, C.R. Formation and growth of humins via aldol addition and condensation during acid-catalyzed conversion of 5-hydroxymethylfurfural. *Energy Fuels* **2011**, *25*, 4745–4755. [CrossRef]
32. Carniti, P.; Gervasini, A.; Bossola, F.; Dal Santo, V. Cooperative action of Brønsted and Lewis acid sites of niobium phosphate catalysts for cellobiose conversion in water. *Appl. Catal. B Environ.* **2016**, *193*, 93–102. [CrossRef]
33. Sing, K.S.W.; Everett, D.H.; Haul, R.A.W.; Moscou, R.A.; Pierotti, R.; Rouquerol, J.; Siemieniewska, T. Reporting physisorption data for gas/solid systems. In *Handbook of Heterogeneous Catalysis*, 1st ed.; Wiley-VCH Verlag GmbH & Co: Weinheim, Germany, 2008; Volume 1, pp. 1217–1230. [CrossRef]
34. Gliozzi, G.; Innorta, A.; Mancini, A.; Bortolo, R.; Perego, C.; Ricci, M.; Cavani, F. Zr/P/O catalyst for the direct acid chemo-hydrolysis of non-pretreated microcrystalline cellulose and softwood sawdust. *Appl. Catal. B Environ.* **2014**, *145*, 24–33. [CrossRef]
35. Shimizu, K.; Furukawa, H.; Kobayashi, N.; Itaya, Y.; Satsuma, A. Effects of Brønsted and Lewis acidities on activity and selectivity of heteropolyacid-based catalysts for hydrolysis of cellobiose and cellulose. *Green Chem.* **2009**, *11*, 1627–1632. [CrossRef]
36. Di Fidio, N.; Raspolli Galletti, A.M.; Fulignati, S.; Licursi, D.; Liuzzi, F.; De Bari, I.; Antonetti, C. Multi-Step exploitation of raw *Arundo donax* L. for the selective synthesis of second-generation sugars by chemical and biological route. *Catalysts* **2020**, *10*, 79. [CrossRef]
37. Di Fidio, N.; Ragaglini, G.; Dragoni, F.; Antonetti, C.; Raspolli Galletti, A.M. Integrated cascade biorefinery processes for the production of single cell oil by *Lipomyces starkeyi* from *Arundo donax* L. hydrolysates. *Bioresource Technology* **2021**, *325*, 124635. [CrossRef]
38. Zhang, Z.; Zhu, Z.; Shen, B.; Liu, L. Insights into biochar and hydrochar production and applications: A review. *Energy* **2019**, *171*, 581–598. [CrossRef]
39. Kamiya, Y.; Sakata, S.; Yoshinaga, Y.; Ohnishi, R.; Okuhara, T. Zirconium phosphate with a high surface area as a water-tolerant solid acid. *Catal. Lett.* **2004**, *94*, 45–47. [CrossRef]
40. Sluiter, A.; Hames, B.; Ruiz, R.; Scarlata, C.; Sluiter, J.; Templeton, D.; Crocker, D. *Determination of Structural Carbohydrates and Lignin in Biomass*; NREL/TP-510-42618; National Renewable Energy Laboratory: Golden, CO, USA, 2008; Volume 1617, pp. 1–16.